





Anoxia decreases the magnitude of the carbon, nitrogen, and phosphorus sink in freshwaters

Cayelan C. Carey¹  | Paul C. Hanson²  | R. Quinn Thomas^{1,3}  |
 Alexandra B. Gerling¹  | Alexandria G. Hounshell¹  | Abigail S. L. Lewis¹  |
 Mary E. Lofton¹  | Ryan P. McClure¹  | Heather L. Wander¹  |
 Whitney M. Woelmer¹  | B. R. Niederlehner¹  | Madeline E. Schreiber⁴ 

¹Department of Biological Sciences,
Virginia Tech, Blacksburg, Virginia, USA

²Center for Limnology, University of
Wisconsin-Madison, Madison, Wisconsin,
USA

³Department of Forest Resources and
Environmental Conservation, Virginia
Tech, Blacksburg, Virginia, USA

⁴Department of Geosciences, Virginia
Tech, Blacksburg, Virginia, USA

Correspondence

Cayelan C. Carey, Department of
Biological Sciences, Virginia Tech,
Blacksburg, Virginia 24061, USA.
Email: cayelan@vt.edu

Funding information

Fralin Life Sciences Institute; Institute for
Critical Technology and Applied Science;
National Science Foundation, Grant/
Award Number: DGE-1651272, DBI-
1933102, DBI-1933016, CNS-1737424,
DEB-1753657, DEB-1753639, DEB-
1753657 and DEB-1753639; Virginia Tech
Global Change Center; Western Virginia
Water Authority

Abstract

Oxygen availability is decreasing in many lakes and reservoirs worldwide, raising the urgency for understanding how anoxia (low oxygen) affects coupled biogeochemical cycling, which has major implications for water quality, food webs, and ecosystem functioning. Although the increasing magnitude and prevalence of anoxia has been documented in freshwaters globally, the challenges of disentangling oxygen and temperature responses have hindered assessment of the effects of anoxia on carbon, nitrogen, and phosphorus concentrations, stoichiometry (chemical ratios), and retention in freshwaters. The consequences of anoxia are likely severe and may be irreversible, necessitating ecosystem-scale experimental investigation of decreasing freshwater oxygen availability. To address this gap, we devised and conducted REDOX (the Reservoir Ecosystem Dynamic Oxygenation eXperiment), an unprecedented, 7-year experiment in which we manipulated and modeled bottom-water (hypolimnetic) oxygen availability at the whole-ecosystem scale in a eutrophic reservoir. Seven years of data reveal that anoxia significantly increased hypolimnetic carbon, nitrogen, and phosphorus concentrations and altered elemental stoichiometry by factors of 2–5x relative to oxic periods. Importantly, prolonged summer anoxia increased nitrogen export from the reservoir by six-fold and changed the reservoir from a net sink to a net source of phosphorus and organic carbon downstream. While low oxygen in freshwaters is thought of as a response to land use and climate change, results from REDOX demonstrate that low oxygen can also be a *driver* of major changes to freshwater biogeochemical cycling, which may serve as an intensifying feedback that increases anoxia in downstream waterbodies. Consequently, as climate and land use change continue to increase the prevalence of anoxia in lakes and reservoirs globally, it is likely that anoxia will have major effects on freshwater carbon, nitrogen, and phosphorus budgets as well as water quality and ecosystem functioning.

KEYWORDS

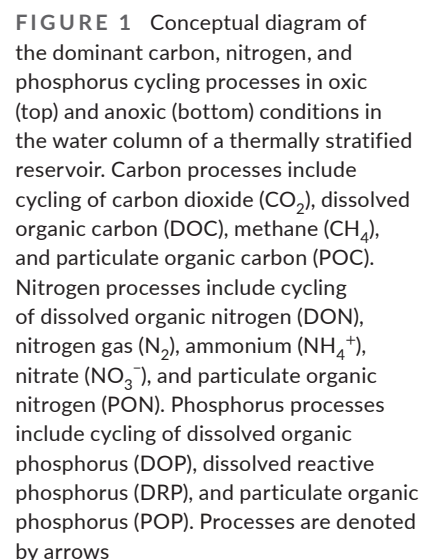
biogeochemistry, ecosystem modeling, hypoxia, nutrient retention, oxygen, REDOX, reservoir, stoichiometry, water quality, whole-ecosystem experiment

This is an open access article under the terms of the [Creative Commons Attribution-NonCommercial](https://creativecommons.org/licenses/by-nc/4.0/) License, which permits use, distribution and reproduction in any medium, provided the original work is properly cited and is not used for commercial purposes.

© 2022 The Authors. *Global Change Biology* published by John Wiley & Sons Ltd.

Oxygen concentrations in lakes and reservoirs around the world are decreasing, which has the potential to substantially alter freshwater ecosystem functioning and water quality. As a result of climate and land use change, low oxygen availability (anoxia) is becoming more common in the hypolimnion, or bottom waters, of many lakes and reservoirs (Jane et al., 2021; Jenny, Francus, et al., 2016; Woolway et al., 2021). An increase in both the occurrence and duration of hypolimnetic anoxia in freshwaters is likely to substantially alter the cycles of carbon (C), nitrogen (N), and phosphorus (P), three fundamental elements that determine freshwater food web structure, water quality, and ecosystem functioning (Kortelainen et al., 2013; Sterner & Elser, 2002). In particular, anoxia could disrupt the critical role of freshwater ecosystems as C, N, and P sinks in global biogeochemical cycles. Freshwaters retain 72% of the total organic C, 56% of the total N, and 56% of the total P exported from land via sediment burial or release to the atmosphere, preventing these elements from being transported to downstream freshwater ecosystems or the oceans (Maranger et al., 2018). Altogether, the consequences of anoxia for C, N, and P concentrations, stoichiometry (chemical ratios), and retention in freshwaters are likely severe and may be irreversible (Brothers et al., 2014; North et al., 2014; Nürnberg, 1988;

Biogeochemical cycles of dissolved and total C, N, and P will likely respond differently to hypolimnetic anoxia (Figure 1). In the bottom waters of lakes and reservoirs, we expect dissolved organic C (DOC) concentrations to be higher in anoxic than oxic conditions, as DOC is mineralized much more efficiently by oxygen than by alternate terminal electron acceptors (Beutel, 2003; Walker & Snodgrass, 1986). Moreover, anoxia has been shown to stimulate the release of DOC from sediments to the water column (Figure 1; Brothers et al., 2014; Peter et al., 2017), as well as increase hypolimnetic methane concentrations and subsequent greenhouse gas emissions (Bartosiewicz et al., 2019; Hounshell et al., 2021; Vachon et al., 2019). DOC generally dominates the total OC (TOC) pool in lakes (Toming et al., 2020), thus we would expect TOC to exhibit similar responses as DOC to anoxia. For hypolimnetic dissolved inorganic nitrogen (DIN), ammonium (NH_4^+) concentrations would be expected to be higher in anoxic conditions due to ammonification and release from sediments (Figure 1; Beutel et al., 2006; Rysgaard et al., 1994). In contrast, nitrate (NO_3^-) would be lower in anoxic than oxic conditions, as denitrification decreases NO_3^- in the absence of oxygen while nitrification increases NO_3^- in the presence of oxygen (Figure 1; Downes, 1987;



Sharma & Ahlert, 1977). Total nitrogen (TN) in the hypolimnion could either increase or decrease in anoxic conditions, depending on the balance of NH_4^+ versus NO_3^- within the DIN pool, as the inorganic fraction of hypolimnetic dissolved N is generally greater than the organic fraction (Kim et al., 2006). For hypolimnetic phosphorus (P), we would expect that dissolved reactive phosphorus (DRP) concentrations would be higher in anoxic conditions as DRP is released into the water column during iron reduction and particulate organic matter mineralization (Figure 1; Boström et al., 1988; Mortimer, 1971; Nürnberg, 1988; Rydin, 2000). Total P (TP) concentrations would likely exhibit a similar but more muted response to anoxia than DRP, as DRP is usually a small fraction of the TP pool (Wetzel, 2001).

While these different C, N, and P processes have been well-studied individually, there have been no studies on the net effect of anoxia on all of these cycles operating concurrently at the ecosystem scale, likely due to the challenges of disentangling complex coupled biogeochemical cycling with observational field studies or laboratory experiments. Explicitly considering interconnected elemental cycles and their stoichiometry (following Sterner & Elser, 2002) is essential to understanding the effects of anoxia on ecosystem functioning.

Increases in hypolimnetic anoxia have substantial implications for the fate of C, N, and P in freshwater ecosystems. There are two primary fates for C, N, and P entering into a waterbody: (1) retention, by either remaining in the water column, burial in the sediments, or emission to the atmosphere (for C and N only); or (2) export downstream (following the ecosystem retention definition used by Dillon & Molot, 1997; Harrison et al., 2009; Maranger et al., 2018; Powers et al., 2015, and many others). Anoxia may decrease the ability of lakes and reservoirs to retain NH_4^+ and DRP by reducing their burial in sediments (North et al., 2014; Powers et al., 2015; Rysgaard et al., 1994), thereby increasing their downstream export. Conversely, anoxia could increase the retention of NO_3^- by increasing its emission to the atmosphere via denitrification, thereby decreasing its downstream export (Figure 1; Beaulieu et al., 2014). For C, the ecosystem-scale effects of anoxia are likely complex. The TOC pool includes dissolved and particulate fractions of OC that may respond to oxygen differently and are mediated by ambient environmental conditions, such as external loading, temperature, nutrients, and light (Hanson et al., 2015). For example, anoxia could increase the retention of particulate OC (POC) by decreasing its mineralization, thereby potentially increasing its burial in sediments (Beutel, 2003; Walker & Snodgrass, 1986). Simultaneously, anoxia could decrease the retention of DOC by stimulating fluxes of DOC from the sediments into the water column (e.g., by reductive dissolution of iron-bound DOC complexes; Skoog & Arias-Esquivel, 2009), thereby potentially decreasing burial in sediments (Brothers et al., 2014; Peter et al., 2017), and increasing DOC export downstream. Consequently, quantifying the net effects of anoxia on C, N, and P retention versus downstream export (and thus determining if a waterbody is a sink or source of C, N, and P downstream) is needed to improve our understanding of the changing role of lakes and reservoirs in global biogeochemical cycles.

In particular, human-made reservoirs, which retain substantially more inflowing C, N, and P per unit area than naturally formed lakes globally via either sediment burial or emissions to the atmosphere (Harrison et al., 2009; Maranger et al., 2018; Powers et al., 2016), may be very sensitive to the effects of hypolimnetic anoxia. Despite only covering 6%–11% of the global lentic surface (Downing et al., 2006; Lehner et al., 2011; Verpoorter et al., 2014), reservoirs alone are estimated to account for ~40% of total annual global OC burial (Mendonça et al., 2017) and 26% of total annual global P burial (Maranger et al., 2018). Moreover, reservoirs globally emit $6.5 \text{ TgN year}^{-1}$ to the atmosphere, primarily via denitrification (Beusen et al., 2016; Harrison et al., 2009). In an analysis of ~1000 lakes and reservoirs sampled once across the U.S., reservoirs were found to have lower organic C:P and N:P ratios than naturally formed lakes, which was attributed in part to a greater incidence of hypolimnetic anoxia in reservoirs than naturally formed lakes (Maranger et al., 2018). However, that study lacked accompanying oxygen data to examine how C, N, and P varied across a gradient of oxygen availability. Moreover, the amalgamation of data from waterbodies with different climate and catchment land use makes it challenging to quantify how changing oxygen alters water column C, N, and P concentrations, stoichiometry, and export. We need new approaches that embrace the dynamic nature of reservoirs over time and allow us to disentangle the effects of hypolimnetic anoxia on these waterbodies, especially as their construction is increasing globally (Zarfl et al., 2015).

To mechanistically quantify the effects of anoxia on C, N, and P cycling, we devised and conducted REDOX (the Reservoir Ecosystem Dynamic Oxygenation eXperiment), an unprecedented, 7-year study that integrated a long-term hypolimnetic oxygenation manipulation with ecosystem modeling in a eutrophic reservoir. Coupled whole-ecosystem manipulations and ecosystem modeling provide a powerful approach for both quantifying the effects of hypolimnetic anoxia on C, N, and P cycling and testing the mechanisms underlying continental-scale patterns derived from thousands of waterbodies (e.g., Helton et al., 2015; Maranger et al., 2018). Foundational work based on sediment core incubations in the laboratory and small chambers placed in situ on the sediments of lakes and reservoirs (e.g., Frindte et al., 2015; Lau et al., 2016) have yet to be tested at the ecosystem scale, which is needed to overcome the limitations of small volumes of water and mesocosm fouling. Studies that manipulate an entire ecosystem are able to disentangle the effects of oxygen availability from other environmental drivers, such as water temperature and biological activity, on C, N, and P cycling (Cole, 2013). However, it is logistically challenging to replicate these intensive experiments under different meteorological and environmental conditions over time to assess robustness and repeatability of ecosystem responses. Consequently, data from whole-ecosystem manipulations can be used to calibrate ecosystem models (following Medlyn et al., 2015) that can simulate complex ecosystem responses under a range of oxygen scenarios and weather conditions over multiple years, thereby overcoming the constraints of separate empirical and model investigations.

The purpose of REDOX was to study ecosystem-scale functioning under contrasting oxygen conditions over multiple years in the same reservoir. First, we intensively monitored dissolved oxygen and total and dissolved C, N, and P chemistry, as well as a suite of accompanying water quality variables, in the reservoir during the 7-year field manipulation. Second, we used the empirical data to calibrate a coupled hydrodynamic-ecosystem model, which was used to quantify the effects of varying oxygen conditions over the 7 years. To further investigate changes in reservoir C, N, and P cycling due to anoxia, we used the calibrated model to test hypolimnetic oxygen scenarios under a range of seasonal and meteorological conditions. We focused on two contrasting model scenarios: one in which there was oxygenation throughout the stratified summer period in all 7 years, resulting in continuous oxic conditions, and one in which there was no oxygenation, resulting in hypolimnetic anoxia every summer. We used the model output to address the following questions: (Q1) How does hypolimnetic oxygen availability affect total and dissolved C, N, and P concentrations and stoichiometry?, and (Q2) How does hypolimnetic anoxia affect reservoir retention and downstream export of C, N, and P?

2 | MATERIALS AND METHODS

2.1 | Site description

We studied the effect of changing oxygen conditions on C, N, and P dynamics in Falling Creek Reservoir (FCR), a small eutrophic reservoir located in Vinton, Virginia, USA (37.303479, -79.837371; Figure 2). FCR has a maximum depth of 9.3 m and surface area of 0.119 km² and is a drinking water source operated by the Western Virginia Water Authority (WVWA; Gerling et al., 2014). FCR's watershed was farmland at the time of reservoir construction in 1898 and is almost completely deciduous forest today following agricultural abandonment in the 1930s (Gerling et al., 2016). The reservoir has never been dredged (Gerling et al., 2016), and had a mean hydraulic residence time of 281 days (± 12 days, 1 SE) during our study. FCR has hypolimnetic outtake valves from which water can be withdrawn for treatment.

2.2 | Whole-ecosystem manipulations

We manipulated hypolimnetic oxygen availability in FCR using an engineered hypolimnetic oxygenation system (HOx) deployed by the WVWA in 2012, which allowed us to generate contrasting summer oxic and anoxic conditions (Gerling et al., 2014). The HOx system withdraws hypolimnetic water from 8 m depth, injects dissolved oxygen into the water at super-saturated concentrations onshore, and returns the oxygenated water back to the hypolimnion at 8 m without altering thermal stratification or water temperature (Gerling et al., 2014).

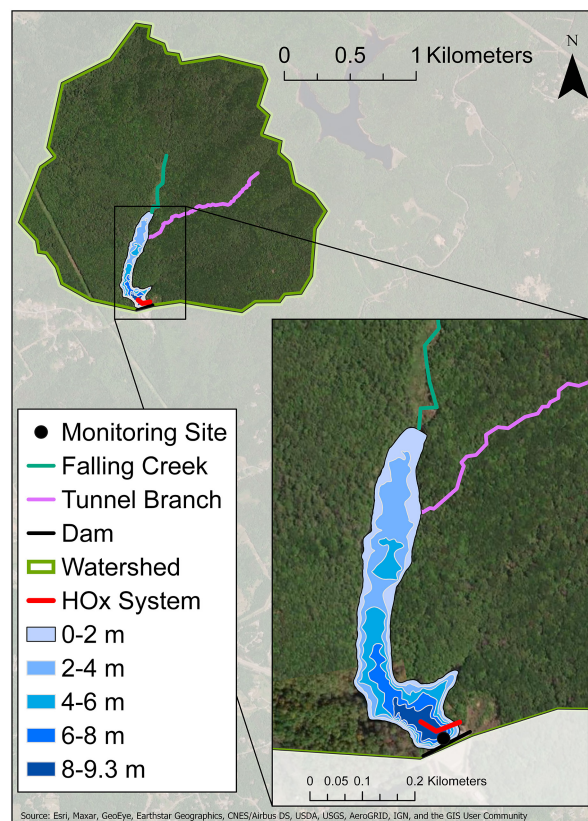


FIGURE 2 Map of Falling Creek Reservoir, Vinton, VA, USA (37.303479, -79.837371). The map shows the reservoir watershed, locations of the two inflow streams (Falling Creek and Tunnel Branch), dam, hypolimnetic oxygenation (HOx) system, and monitoring site near the dam

During the summers of 2013–2019, the HOx system was operated at variable oxygen addition levels and durations in collaboration with the WVWA (Carey, Thomas, & Hanson, 2022). Some summers experienced intermittent 4-week periods of oxygenation (2013, 2014), some summers had near-continuous oxygenation (2015, 2016, 2017), one summer had approximately half oxygenation (2018), and one summer experienced intermittent 2-week periods of oxygenation (2019; Carey, Thomas, & Hanson, 2022). These wide-ranging oxygenation conditions, which occurred because the reservoir was an actively managed drinking water source, provided an ideal dataset for calibrating the biogeochemical rates in the ecosystem model to variable hypolimnetic oxygen conditions, as described below.

2.3 | Monitoring data

FCR's physics, chemistry, and biology were intensively monitored throughout the REDOX manipulations (see Supporting Information Text 1 for detailed field sampling methods). On every sampling day, depth profiles of water temperature and dissolved oxygen were collected at the deepest site of the reservoir, near the dam (Carey, Lewis, et al., 2021). We collected water samples for total and dissolved N, P, and organic C (hereafter, C) analyses

from the reservoir's water treatment extraction depths (0.1, 1.6, 2.8, 3.8, 5.0, 6.2, 8.0, and 9.0 m) using a Van Dorn sampler. Water was filtered through glass-fiber 0.7-micron filters into acid-washed bottles and immediately frozen until analysis for dissolved C, N, and P samples (Carey, Wander, et al., 2021). Unfiltered water was frozen in separate acid-washed bottles for total samples (Carey, Wander, et al., 2021). We focused our sampling and analysis on organic C, rather than inorganic C, because of the important role of reservoirs in burying this pool in the global C cycle (Mendonça et al., 2017), and because previous work indicates that most terrestrial dissolved inorganic C loads are rapidly emitted to the atmosphere (McDonald et al., 2013).

We used standard methods for biogeochemical analyses (see Supporting Information Text 2 for detailed laboratory methods). We used flow injection analysis to determine concentrations of N and P colorimetrically (APHA, 2017), with an alkaline persulfate digestion for TN and TP fractions. DOC and TOC were determined by either heated persulfate digestion or high-temperature combustion followed by infrared absorbance (APHA, 2017; see Table S1). All field and laboratory data are available with detailed metadata in the Environmental Data Initiative (EDI) repository (Carey et al., 2019, 2020; Carey, Hounshell, et al., 2021; Carey, Lewis, et al., 2021; Carey, Wander, et al., 2021; Carey, Wynne, et al., 2021).

2.4 | Model description and driver data

We used the empirical data to calibrate and validate the General Lake Model coupled to Aquatic EcoDynamics modules (GLM-AED, v.3.2.0a3) configured for FCR (see Supporting Information Text 3 for detailed modeling methods). GLM-AED is an open-source, 1-D numerical simulation model that is widely used in the freshwater research community to model lakes and reservoirs (e.g., Bruce et al., 2018; Farrell et al., 2020; Hipsey, 2022; Hipsey et al., 2019; Ward et al., 2020). GLM-AED requires meteorological, inflow, and outflow driver data and simulates water balance and thermal layers using a Lagrangian strategy (Hipsey, 2022; Hipsey et al., 2019). GLM-AED has a flexible structure in which modules representing different ecosystem components can be turned on or off to recreate varying levels of ecosystem complexity; our configuration for FCR included modules for oxygen, C, silica (Si), N, P, organic matter, and phytoplankton (Carey, Thomas, & Hanson, 2022; Carey, Thomas, McClure, et al., 2022).

GLM-AED simulates the dominant processes controlling freshwater oxygen and C, N, and P cycling (see Supporting Information Text 3; Hipsey, 2022). Biogeochemical processes (e.g., sediment fluxes, mineralization) were modeled as a function of both oxygen following Michaelis-Menten dynamics and temperature following Arrhenius coefficients (Farrell et al., 2020). Consequently, processes that are favored in anoxic conditions (e.g., sediment fluxes of DOC, NH_4^+ , and DRP into the hypolimnion) were still simulated in oxic conditions, but at much lower rates.

The ecosystem model provided important insight on the effects of anoxia that would have been impossible to obtain from the field manipulation alone. First, while we do report on the biogeochemical responses to the field manipulation to provide complementary data to the model output, ecosystems rarely experience such rapid shifts in redox conditions at sub-seasonal scales, as were created by abrupt additions of oxygen via the HOx system. Thus, to understand how our FCR results applied to other waterbodies, we used the 7-year field manipulation as a proxy to contrast the consequences of seasonally oxic versus anoxic hypolimnia for biogeochemical cycling in an ecosystem model. These highly contrasting scenarios were achieved in the model by manipulating hypolimnetic oxygen injection (described below). Second, to determine the cumulative fate of C, N, and P over an entire summer in response to oxygen dynamics, it is important to track these elements at a high temporal resolution. Because our field data were collected weekly to monthly, we used numerical modeling of hydrodynamics and ecosystem processes to capture daily dynamics. Third, the field manipulation included a variable oxygenation schedule which occurred against a backdrop of changing meteorology and hydrology. Consequently, the model enabled us to isolate the effects of oxygen availability on the reservoir's biogeochemistry and evaluate the robustness of ecosystem responses across varying environmental conditions.

2.5 | Model configuration and calibration

All GLM-AED model configuration files, parameters, and driver data for FCR are available in the EDI repository (Carey, Thomas, & Hanson, 2022). GLM-AED driver data included hourly meteorological data from NASA's North American Land Data Assimilation System (NLDAS-2; Xia et al., 2012), stream inflow data, and outflow data. We developed stream inflow driver datasets—which consisted of daily discharge, water temperature, and chemistry—for the two primary streams entering FCR from observational data (Supporting Information Text 3). To simulate the HOx system in the model, we added a submerged inflow that injected oxygenated water into the reservoir at 8 m, the same depth as in the reservoir. As the reservoir was managed to keep constant water level, outflow volume was set to equal inflow volume; the physical and chemical properties of the outflow were determined by the state of the modeled reservoir (Supporting Information Text 3).

We ran the model from May 15, 2013 to December 31, 2019, divided into calibration (May 15, 2013–December 31, 2018) and validation (January 1, 2019–December 31, 2019) periods for model verification. GLM-AED was run on an hourly time step throughout the total simulation period (Carey, Thomas, & Hanson, 2022).

We calibrated GLM-AED to observed conditions (Supporting Information Text 3). First, we conducted a global sensitivity analysis to identify the most important parameters for simulating water temperature, dissolved oxygen, NH_4^+ , NO_3^- , DRP, and DOC following Morris (1991). Second, we calibrated the identified sensitive parameters (Table S2) using the covariance matrix

adaptation evolution strategy for automated numerical optimization (Hansen, 2016) to minimize root mean square error (RMSE) between observations and model output for all sampling depths in the water column.

We calculated multiple goodness-of-fit metrics to assess the model's performance during the calibration period, validation period, and total simulation period, including RMSE, the coefficient of determination (R^2), percent bias, and normalized mean absolute error (NMAE) (e.g., Kara et al., 2012; Ladwig et al., 2021; Ward et al., 2020). We calculated these goodness-of-fit metrics following the most common approaches used in 328 recent freshwater modeling studies (reviewed by Soares & Calijuri, 2021; described in Supporting Information Text 3).

2.6 | Model scenarios

Following model calibration, we examined the effects of two different oxygen scenarios on FCR's biogeochemistry using the GLM-AED model: (1) an "oxic" scenario in which the model was forced with a high level of oxygenation to keep the hypolimnion oxic throughout summer thermal stratification (May 15–October 15) during 2013–2019; and (2) an "anoxic" scenario in which zero oxygen was added to the hypolimnion, so hypolimnetic anoxia quickly set up after the onset of thermal stratification each summer. All other driver data (meteorology, stream inflows, outflow) were held constant.

2.7 | Statistical analysis

We used several approaches to answer the two research questions. For Q1, we first compared observed data from the oxygenated versus non-oxygenated periods of our field manipulation to determine if oxygenation had an effect on empirical total and dissolved C, N, and P concentrations. We pooled all hypolimnetic C, N, and P samples from the two summers with the least oxygenation (July 15–October 1 in 2018, 2019) when the HOx was deactivated and compared them with concentrations measured during the two summers with the most continuous oxygenation (July 15–October 1 in 2016, 2017) when the HOx was activated (Supporting Information Text 4). We also used the FCR field data to validate the model's ability to simulate the field manipulation. Second, because our goal was to compare completely oxic versus completely anoxic summers and every summer had at least some oxygenation during the 7-year field manipulation, we focused our subsequent analyses on the anoxic versus oxic model scenario output, which provided complementary data to the non-oxygenated versus oxygenated empirical data. Focusing on the model output for this analysis also enabled us to overcome the limitations of comparing years with different numbers of sampling observations, as the model calculated daily C, N, and P concentrations and rates.

We compared hypolimnetic C, N, and P concentrations and rates between the oxic and anoxic model scenarios during July 15–October 1 among years, the interval within the summer thermally stratified period when the reservoir consistently exhibited hypolimnetic anoxia in non-oxygenated conditions. We calculated the median hypolimnetic dissolved and total concentrations of C, N, and P during this period for each of the 7 years (2013–2019), and compared the median summer anoxic and oxic concentrations and their ratios using paired *t*-tests, as there was no temporal autocorrelation among median summer values (Supporting Information Text 5). We also examined summer rates of all processes controlling increases and decreases in hypolimnetic C, N, and P to determine their relative importance and sensitivity to oxygen.

To examine how the uncertainty of our model outputs was affected by the model parameterization, we conducted an additional sensitivity analysis in which we doubled and halved the calibrated values of highly sensitive parameters for DOC, NH_4^+ , NO_3^- , and DRP using a one-step-at-a-time (OAT) approach (following Brett et al., 2016). We then re-calculated the summer hypolimnetic concentrations of DOC, NH_4^+ , NO_3^- , and DRP in the anoxic and oxic model scenarios for each variable and compared anoxic and oxic concentrations with paired *t*-tests, as described above (Supporting Information Text 3, Figure S1).

For Q2, we estimated C, N, and P downstream export as a percent of inputs into the reservoir each summer (Farrell et al., 2020; Powers et al., 2015). Downstream export was calculated as:

$$\text{Flux} = 100\% \times ([\Sigma \text{Outputs} - \Sigma \text{Inputs}] / \Sigma \text{Inputs}), \quad (1)$$

where Outputs and Inputs represent the daily mass of C, N, or P leaving and entering the reservoir, respectively, during July 15–October 1 each year. Fluxes were calculated for both dissolved and total fractions of C, N, and P. Inputs were calculated by multiplying the individual stream daily inflow concentrations with their daily inflow volumes and then summing across the two streams. Outputs were calculated by multiplying the outflow water volume (leaving the reservoir and going downstream) by hypolimnetic concentrations. A water budget calculated for the reservoir in 2014–2015 (Munger et al., 2019) supplemented by monitoring data in this study indicates that the two inflow streams represented approximately 97% of the reservoir's water inputs (Supporting Information Text 1), motivating our focus on those inputs.

Inputs and Outputs were summed across the July 15–October 1 period to calculate C, N, and P fluxes. Flux values of 0 indicated that the reservoir inputs balanced outputs; flux values <0 indicated that the reservoir was a net sink of C, N, or P; and flux values >0 indicated that the reservoir was a net source of C, N, or P downstream. We compared summer retention (i.e., flux values) in the anoxic and oxic scenarios with paired *t*-tests (Supporting Information Text 5).

To ease comparison among C, N, and P concentrations and ratios, all analyses were conducted in molar units. All analyses were conducted in R v.3.6.3 (R Core Team, 2020) and all code to reproduce

these analyses is available in the Zenodo repository (Carey, Thomas, McClure, et al., 2022).

3 | RESULTS

Our integrated whole-ecosystem REDOX field manipulation and modeling demonstrates that hypolimnetic anoxia significantly alters water column C, N, and P concentrations and stoichiometry. Importantly, our study also shows that prolonged hypolimnetic anoxia in the summer decreases the ability of a reservoir to retain C, N, and P, substantially increasing the downstream export of these elements.

3.1 | Observational data from whole-ecosystem manipulations

Injection of oxygen into the bottom waters of Falling Creek Reservoir (FCR) over 7 years increased the reservoir's observed hypolimnetic oxygen, resulting in substantial changes in total and dissolved C, N, and P concentrations (Figure 3, Figure S2). Due to the nature of our oxygenation manipulation, some years experienced low levels of oxygenation (i.e., the HOx was off for prolonged periods throughout the summer), while others experienced high levels of oxygenation during the stratified period (Figure 3b). Oxygenation resulted in substantially higher hypolimnetic oxygen concentrations without altering water temperature and thermal stratification in the reservoir (Figure 3a,b). In 2019, oxygenation did not increase hypolimnetic oxygen concentrations to the same extent as preceding summers, likely because the HOx was only operated for intermittent 2-week periods (vs. 4-week or longer periods in all other years).

The median observed hypolimnetic DOC, NH_4^+ , and DRP concentrations were 2.0, 6.9, and 1.3 \times higher in the summers with the least oxygenation (2018, 2019) than in the summers with the highest oxygenation (2016, 2017; Figure 3c,e,h; Figure S2), respectively. Following the patterns exhibited by the dissolved fractions, median observed hypolimnetic TN and TP concentrations were both 2.4 \times higher in the low versus high oxygenation summers (Figure 3d,g; Figure S2). Conversely, median observed hypolimnetic NO_3^- concentrations were 5 \times lower in summers with low oxygenation than summers with high oxygenation (Figure 3f; Figure S2). Because our goal was to compare completely oxic versus completely anoxic summer conditions and every summer had at least some oxygenation during the 7-year field manipulation at varying levels of oxygen injection, subsequent analyses focused on the anoxic versus oxic model scenario output, described below.

3.2 | Model performance

The field manipulation data were used to calibrate the ecosystem model, which generally reproduced observed water temperature,

oxygen, dissolved and total C, N, and P concentrations, and stoichiometry (Table 1; Figure 3; Figures S3 and S4). Similar to field observations, the simulation of oxygen injection in the model did not substantively alter modeled water temperature or thermocline depth (Table 1, Figure 3a).

Model performance of most state variables in our study (Table 1) exceeded the median goodness-of-fit metrics for recent freshwater modeling studies reported by Soares and Calijuri (2021). For example, our water temperature R^2 was 0.95 for the full 7-year simulation period (vs. 0.94 in Soares & Calijuri, 2021), our dissolved oxygen R^2 was 0.72 (vs. 0.61), our TN was 0.71 (vs. 0.61), and our NH_4^+ R^2 was 0.77 (vs. 0.35). No DOC data were reported by Soares and Calijuri (2021), but our R^2 values ranged from 0.30–0.52 for the full simulation, calibration, and validation periods. Phosphorus had less good fit, but was still reasonable: our TP R^2 was 0.25 for the full 7-year simulation period (slightly lower than the 0.30 reported by Soares & Calijuri, 2021), but the validation period's R^2 for TP was much higher, at 0.85. Similarly, our DRP R^2 was 0.10 for the full 7-year period (vs. 0.32) but the 6-year calibration period had better performance, at an R^2 of 0.24. NO_3^- had an R^2 of 0.27 for the full 7-year modeling period and R^2 of 0.33 for the 6-year calibration period, which was lower than the 0.61 reported by Soares and Calijuri (2021).

Much of the variation in DRP and NO_3^- observations was within the analytical limits of quantitation (Figure 3f,h). Consequently, while the model generally captured seasonal patterns of DRP and NO_3^- , it was simply not possible to reproduce short-term fluctuations in observations below method detection limits. NO_3^- concentrations in particular were extremely low in both field observations and model output (Figure 3f). Throughout the study, NO_3^- was a very minor fraction of TN, representing a median of 0.5% ($\pm 0.9\%$, 1 SD) of TN at all depths in the field data and a median of 0.8% ($\pm 0.9\%$) of TN in the baseline simulation. Subsequently, a lower fit of NO_3^- did not affect the model performance of TN, as evident by its goodness-of-fit metrics (Table 1).

3.3 | How does hypolimnetic oxygen availability affect total and dissolved C, N, and P concentrations and stoichiometry?

Model scenarios show that hypolimnetic anoxia significantly affected all three focal elemental cycles, but that N was the most sensitive (Figures 4 and 5; see Table S3 for statistics). Summer TN molar concentrations in the reservoir were on average 3.0 \times higher in anoxic than oxic conditions, relative to a 1.1 \times increase of TOC and 1.6 \times increase of TP (Figure 5a,c,g). The dissolved fractions accounted for most of the changes in total C, N, and P: following the field data, modeled summer hypolimnetic DOC, NH_4^+ , and DRP concentrations in FCR were on average 1.1, 5.8, and 3.1 \times higher, respectively, during anoxic conditions than in oxic conditions (Figure 5b,e,h). Conversely, hypolimnetic NO_3^- was much lower in anoxic conditions (usually at or just above 0 mmol m $^{-3}$) than oxic conditions, but DIN exhibited an

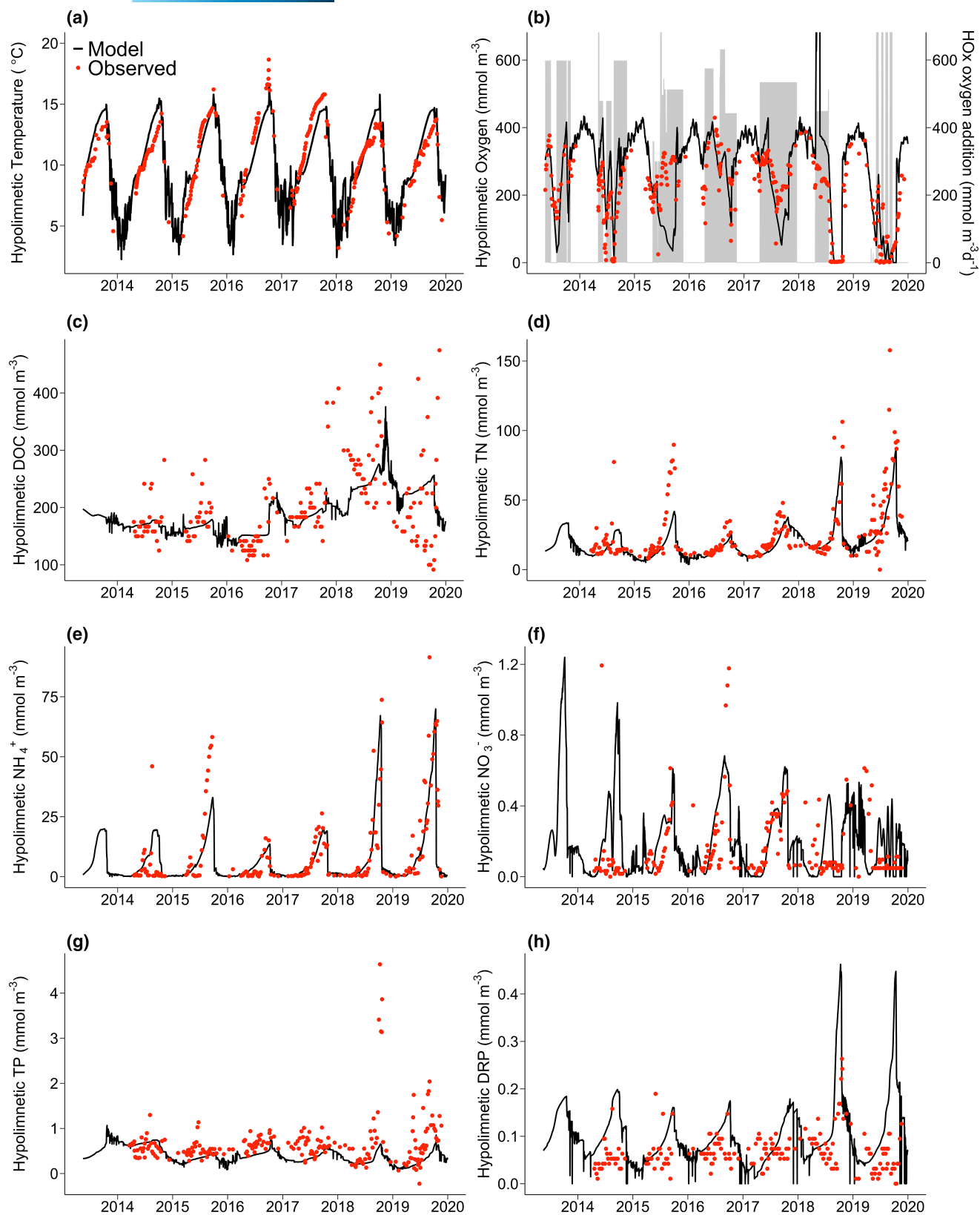


FIGURE 3 The ecosystem model was able to generally recreate observed reservoir dynamics. Modeled (black line) and observed (red points) hypolimnetic (9 m) water temperature (a), dissolved oxygen (b), dissolved organic carbon (DOC; c), total nitrogen (TN; d), ammonium (NH_4^+ ; e), nitrate (NO_3^- ; f), total phosphorus (TP; g), and dissolved reactive phosphorus (DRP; h) in Falling Creek Reservoir (goodness-of-fit metrics presented for the full water column in Table 1). The grey shaded areas in panel (b) represent the periods and addition rates of oxygen injection into the hypolimnion from the hypolimnetic oxygenation system (HOx) during the 7-year field manipulation. Note varying y-axes among panels, and that many of the NO_3^- and DRP observations were below the limits of quantitation in laboratory analysis (0.11 and 0.08 mmol m^{-3} , respectively)

overall increase because of the dominance of NH_4^+ over NO_3^- in the dissolved inorganic N pool (Figure 5d,f). The statistical significance and overall magnitude of differences in concentrations between the anoxic and oxic scenarios were consistent even when focal parameters governing DOC, NH_4^+ , NO_3^- , and DRP were doubled or halved in the parameter sensitivity analysis (Figure S1).

The elemental stoichiometry in FCR exhibited rapid and large ecosystem-scale changes after the onset of anoxia each summer. While total and dissolved fractions of C, N (except NO_3^-), and P significantly increased with anoxia (Figures 4 and 5), the different fractions had varying sensitivities to changing oxygen, resulting in significant changes in C, N, and P ratios (Figure 6; Table S4). Hypolimnetic TN:TP and DIN:DRP were significantly higher (both by 1.9 \times , on average) in anoxic conditions than oxic conditions (Figure 6g,h). Because modeled hypolimnetic NO_3^- concentrations were at or near zero during anoxic conditions (Figure 5f), DOC: NO_3^- could not be consistently calculated (Figure 6e). In contrast, TOC:TN, TOC:TP, DOC:DIN, DOC: NH_4^+ , and DOC:DRP were significantly higher (on average, by 2.7 \times , 0.7 \times , 4.7 \times , 5.0 \times , and 2.7 \times , respectively) in oxic conditions than anoxic conditions (Figure 6a–d,f; Table S4).

The most important processes driving the biogeochemical responses to anoxia were much higher fluxes of NH_4^+ , DRP, and DOC into the hypolimnion from the sediments in anoxic periods relative to oxic periods (Figure 7; Figure S5). During anoxic summer conditions, the median release rates of NH_4^+ and DRP from the sediments into the water column were 3.6 \times and 2.2 \times higher, respectively, than in oxic conditions (Figure 7b,c). During oxic conditions, the sediment release rate of NH_4^+ into the hypolimnion was 34 \times greater than the

consumption of NH_4^+ by nitrification (Figure 7b), thereby explaining the hypolimnetic accumulation of NH_4^+ that occurred during oxic conditions (Figure 4g). Although median labile dissolved organic N (DON) and P (DOP) mineralization rates were both 4.0 \times times higher in oxic than anoxic conditions, their contribution to hypolimnetic N and P budgets was much smaller than NH_4^+ and DRP sediment fluxes. All biogeochemical rates involving the cycling of NO_3^- were much lower than for NH_4^+ overall, likely because of the much lower concentrations of NO_3^- within the DIN pool (Figure 7b). For DOC, the median sediment fluxes increasing DOC in the hypolimnion were 1.9 \times times higher in anoxic than oxic conditions (Figure 7a). Although labile DOC mineralization rates were 2.0 \times higher in oxic than anoxic conditions, sediment flux rates were 19 \times higher than mineralization rates, resulting in greater hypolimnetic accumulation of DOC in anoxic relative to oxic periods (Figure 4d).

The time scales at which C, N, and P concentrations responded to shifts in hypolimnetic oxygen availability differed as a result of multiple interacting biogeochemical processes (Figure 4; Figure 7). For example, the onset of anoxia each summer triggered rapid decreases in NO_3^- (Figure 4h), due to sediment denitrification reducing NO_3^- to N_2 (Figure 7b). Similarly, the rapid increases in hypolimnetic NH_4^+ and DOC concentrations after the onset of anoxia (Figure 4d,g) were attributable to the high rates of NH_4^+ and DOC sediment release (Figure 7a,b). In comparison, hypolimnetic DRP increases in response to anoxia occurred more slowly (Figure 4j). This difference in time scale reflects the lower fitted value of the half-saturation constant of modeled DRP sediment fluxes (6.91 mmol m^{-3}) relative to the half-saturation constants of NH_4^+ sediment fluxes (41.25 mmol m^{-3}).

TABLE 1 Goodness-of-fit (GOF) metrics for comparing observations and modeled GLM-AED output for Falling Creek Reservoir, VA, USA. GOF metrics include root mean square error (RMSE), percent bias (PBIAS%), coefficient of determination (R^2), and normalized mean absolute error (NMAE); n is the number of observed measurements. Each GOF metric was calculated comparing model outputs and observational data for the water column for the full simulation (2013–2019); calibration (2013–2018); and validation (2018–2019); see Supporting Information Text 3 for details. Evaluated parameters include temperature (Temp, °C), summer thermocline depth (TD, m), dissolved oxygen (mmol m^{-3}), dissolved organic carbon (DOC, mmol m^{-3}), total nitrogen (TN, mmol m^{-3}), ammonium (NH_4^+ , mmol m^{-3}), nitrate (NO_3^- , mmol m^{-3}), total phosphorus (TP, mmol m^{-3}), and dissolved reactive phosphorus (DRP, mmol m^{-3})

Time period	Parameter	Temp	TD	Oxygen	DOC	TN	NH_4^+	NO_3^-	TP	DRP
Full simulation	N	3639	324	3726	1277	1518	1277	1485	1724	1271
	RMSE	1.41	0.8	49.1	63.2	5.9	2.81	0.16	0.29	0.05
	PBIAS%	4.4	0.1	6.4	−14.5	−6.2	22.5	9.8	−31.7	26.5
	R^2	0.95	0.50	0.72	0.30	0.71	0.77	0.27	0.25	0.10
	NMAE	0.09	0.18	0.15	0.2	0.22	0.46	0.45	0.38	0.37
Calibration	N	3164	284	3251	1018	1250	1018	1014	1456	1012
	RMSE	1.39	0.9	45.9	61.5	5.0	2.81	0.16	0.25	0.04
	PBIAS%	3.3	−1.4	5.8	−16.8	−0.8	40.7	11.7	−29.6	21.1
	R^2	0.95	0.46	0.71	0.46	0.58	0.63	0.33	0.15	0.24
	NMAE	0.09	0.19	0.14	0.19	0.19	0.61	0.44	0.33	0.28
Validation	N	475	40	475	259	268	259	471	268	259
	RMSE	1.48	0.4	62.8	70.4	9.23	2.79	0.14	0.33	0.08
	PBIAS%	11.2	10.5	9.9	−4.2	−19.8	−7.2	3.3	−42.9	51.6
	R^2	0.97	0.95	0.74	0.52	0.94	0.94	0.12	0.85	0.03
	NMAE	0.12	0.1	0.2	0.24	0.36	0.22	0.49	0.38	0.57

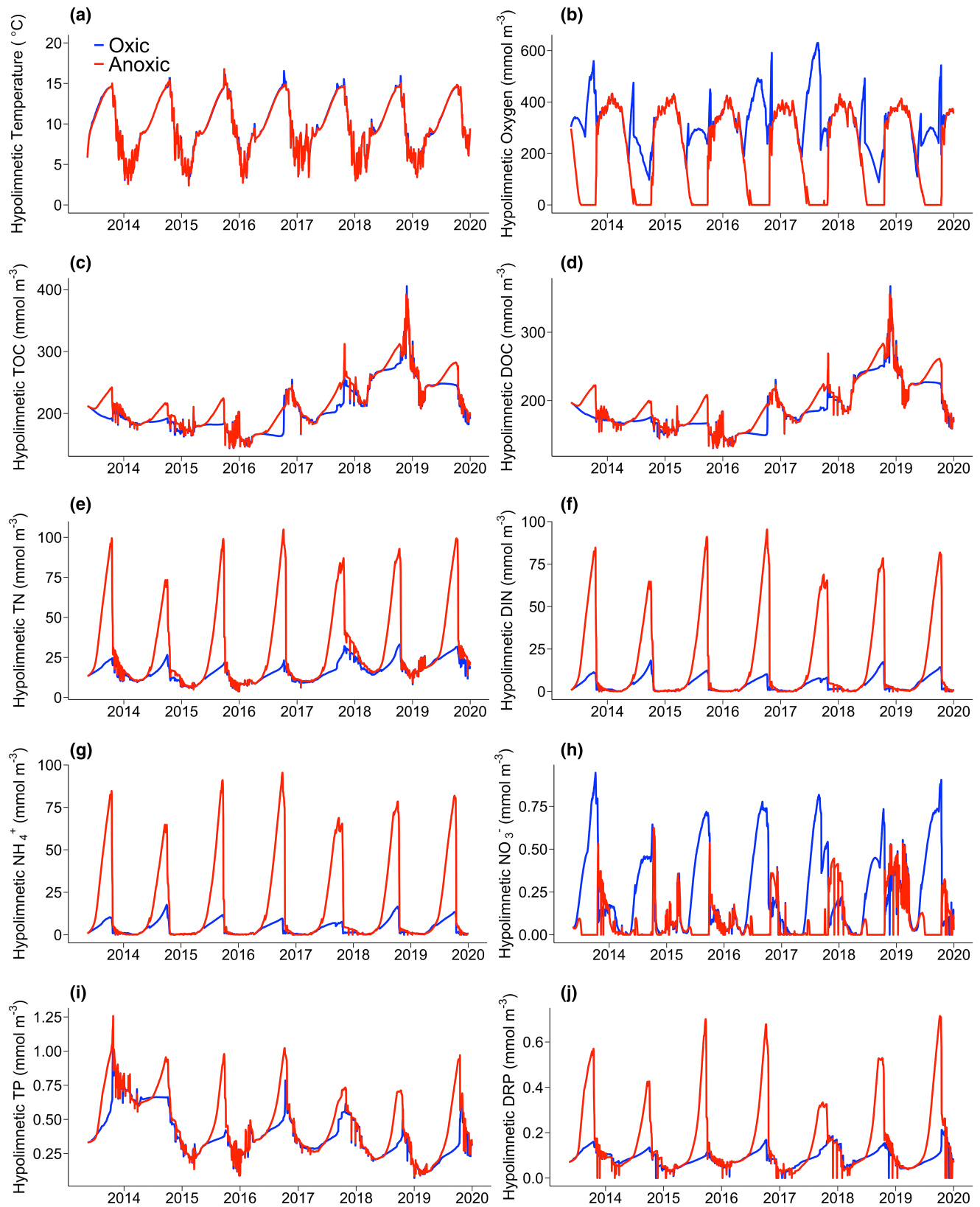


FIGURE 4 Time series of oxic (blue) and anoxic (red) model scenarios in Falling Creek Reservoir. Model results are shown for hypolimnetic (9 m) water temperature (a), dissolved oxygen (b), total organic carbon (TOC; c), dissolved organic carbon (DOC; d), total nitrogen (TN; e), dissolved inorganic nitrogen (DIN, the sum of ammonium and nitrate; f), ammonium (NH_4^+ ; g), nitrate (NO_3^- ; h), total phosphorus (TP; i), and dissolved reactive phosphorus (DRP; j). In the oxic scenario, oxygen was injected into the hypolimnion throughout the thermally stratified period each summer. In the anoxic scenario, no oxygen was added to the hypolimnion, resulting in prolonged hypolimnetic anoxia each summer. Note varying y-axes among panels

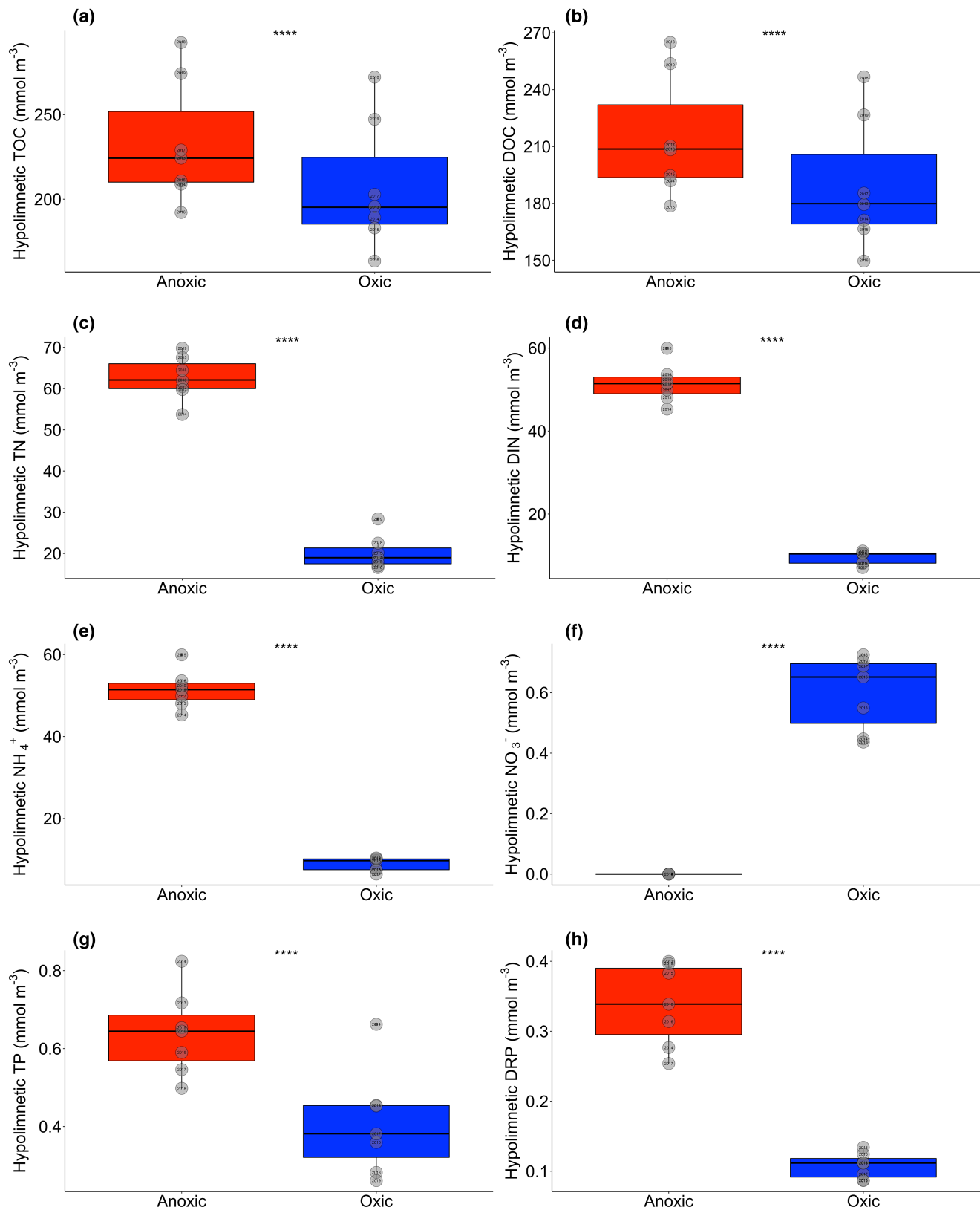


FIGURE 5 Anoxia significantly altered bottom-water concentrations of carbon, nitrogen, and phosphorus. Median hypolimnetic (9 m) total organic carbon (TOC; a), dissolved organic carbon (DOC; b), total nitrogen (TN; c), dissolved inorganic nitrogen (DIN; d), ammonium (NH_4^+ ; e), nitrate (NO_3^- ; f), total phosphorus (TP; g), and dissolved reactive phosphorus (DRP; h) concentrations between anoxic (red) and oxic (blue) scenarios during Falling Creek Reservoir's stratified period (July 15–October 1) for all years of this study. The grey points are the median values from each of the 7 years. The **** denotes that the difference between the median summer anoxic and oxic scenario concentrations was highly statistically significant (all paired t-tests $p \leq .0001$, see Table S3 for statistics). Note varying y-axes among panels

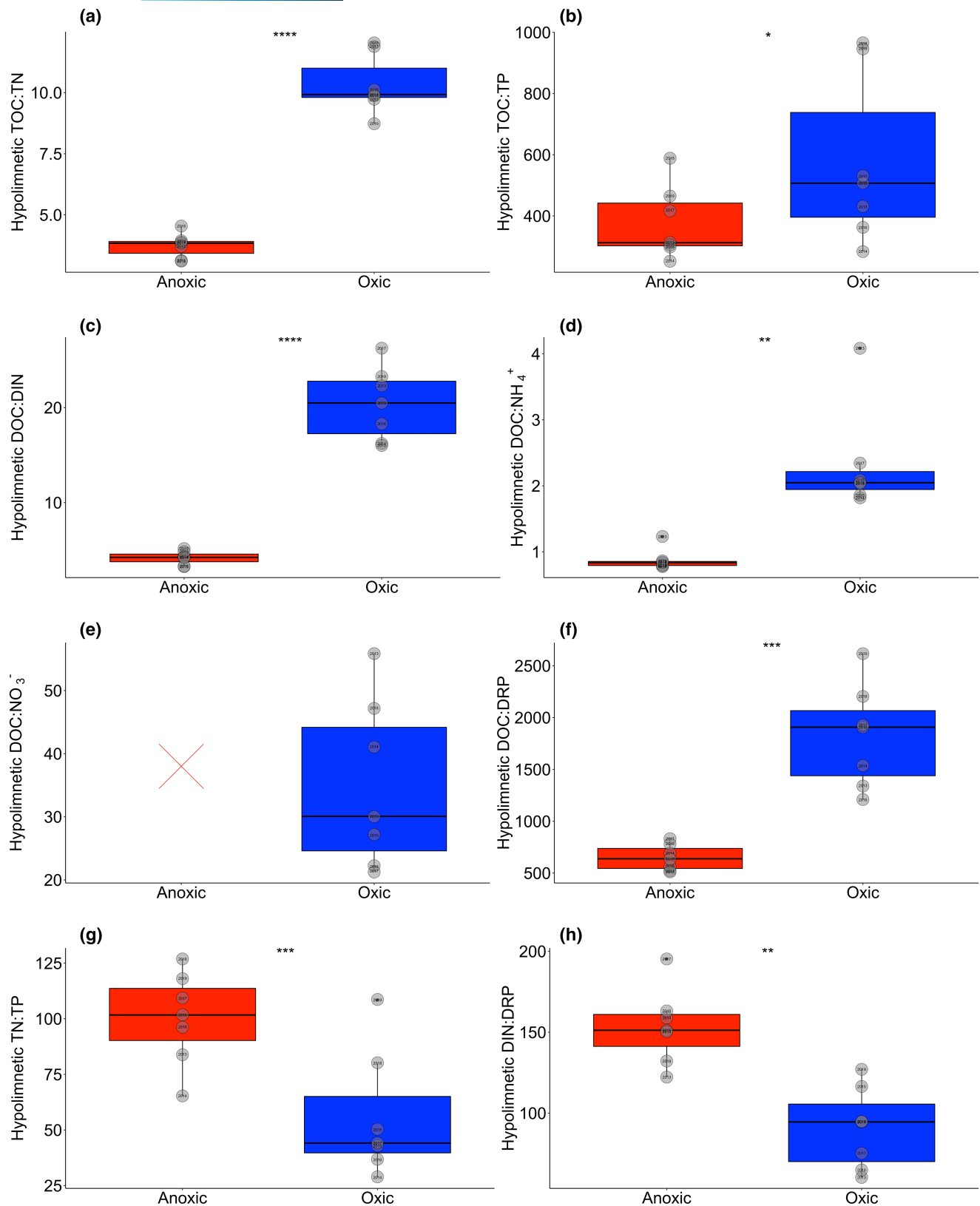
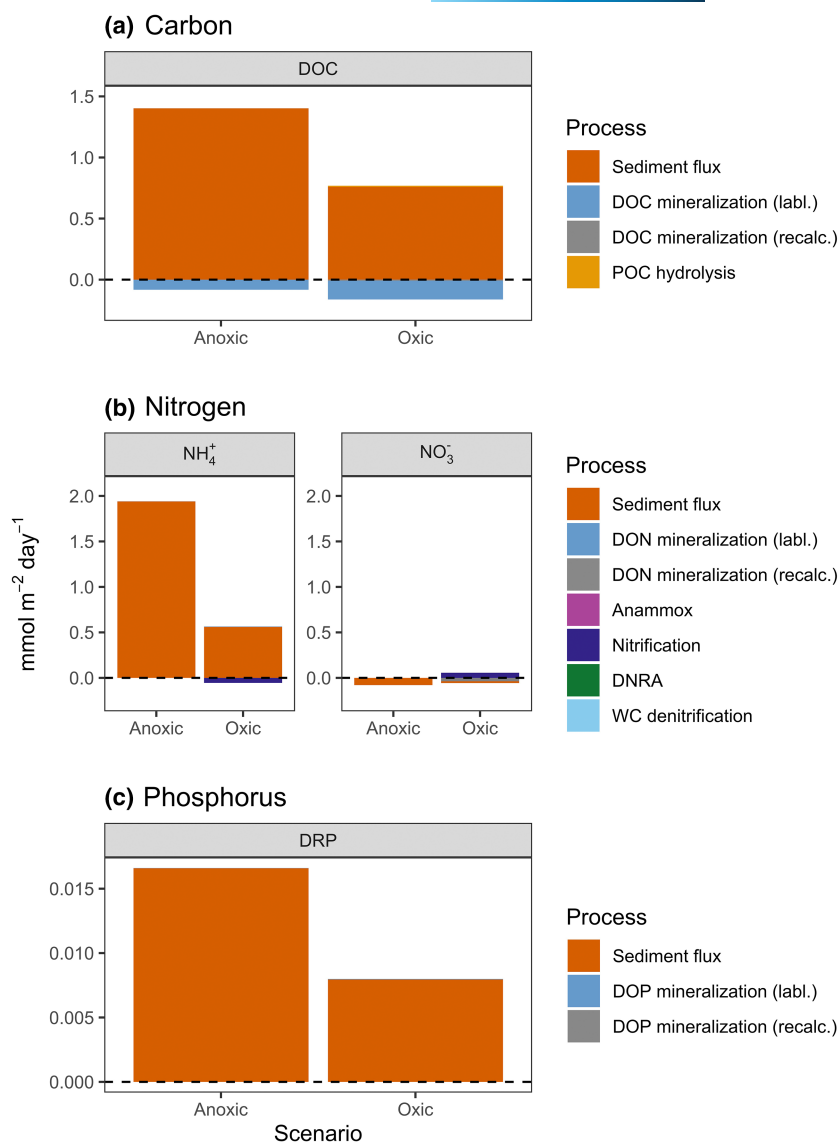


FIGURE 6 Anoxia significantly affected water column stoichiometry. Total and dissolved molar ratios of hypolimnetic (9 m) Total organic carbon: Total nitrogen (TOC:TN; a), TOC:Total phosphorus (TOC:TP; b), Dissolved organic carbon: Dissolved inorganic nitrogen (DOC:DIN; c), DOC:Ammonium (DOC:NH₄⁺; d), DOC:Nitrate (DOC:NO₃⁻; e), DOC:Dissolved reactive phosphorus (DOC:DRP; f), TN:TP (g), and DIN:DRP (h) between anoxic (red) and oxic (blue) scenarios during Falling Creek Reservoir's stratified period (July 15–October 1) for all years of this study. The grey points are the median values from each of the 7 years. Because NO₃⁻ concentrations in the anoxic scenario were functionally zero, the ratio of DOC:NO₃⁻ could not be calculated (hence the X in panel e). The asterisks denote the p -values from paired t -tests comparing the median summer ratios between anoxic and oxic scenarios: **** $p < .0001$, *** $p < .001$, ** $p < .01$, and * $p < .05$ (see Table S4 for statistics). Note varying y -axes among panels

FIGURE 7 Sediment fluxes dominated the responses of dissolved carbon, nitrogen, and phosphorus to anoxia. Comparison of the dominant biogeochemical processes altering dissolved pools of carbon (dissolved organic carbon, DOC; a), nitrogen (ammonium, NH_4^+ , and nitrate, NO_3^- ; b), and phosphorus (dissolved reactive phosphorus, DRP; c) in the hypolimnion of Falling Creek Reservoir under anoxic versus oxic model scenarios. Rates shown represent the median contribution of each process to hypolimnetic concentrations of DOC, NH_4^+ , NO_3^- , and DRP during Falling Creek Reservoir's summer stratified period (July 15–October 1) for all years of this study. Positive rates indicate that the process increased hypolimnetic concentrations; negative rates indicate that the process decreased hypolimnetic concentrations. Mineralization is shown separately for both labile (labl.) and recalcitrant (recalc.) dissolved organic pools, and denitrification is partitioned for the water column (WC denitrification) and sediment in the NO_3^- panel (sediment flux). Note the varying y-axes among panels and that some rates are so small that they are not visible in the figure; Figure S5 shows a modified version of this figure with the sediment fluxes excluded



and DOC sediment fluxes ($93.13 \text{ mmol m}^{-3}$; Carey, Thomas, & Hanson, 2022). Consequently, oxygen concentrations in the hypolimnion had to decrease to near zero before anoxia stimulated an increase in DRP sediment fluxes, following Michaelis–Menten dynamics.

3.4 | How does hypolimnetic anoxia affect reservoir downstream export of C, N, and P?

Overall, anoxia significantly increased downstream export of C, N, and P from FCR (Figure 8). During the summer months, if the reservoir's hypolimnion was oxic, FCR served as a net sink for inflowing TOC and TP, decreasing the downstream export of those fractions (Figure 8a,g). The reservoir served as a particularly important TP sink during summer oxic conditions, with a median of 22% of inflowing TP buried in sediments, resulting in 78% of the inflowing TP exported downstream (Figure 9). In comparison, while the reservoir was also a TOC sink in oxic conditions, only 8% of inflowing TOC was buried in sediments or removed via emission to the atmosphere, resulting

in 92% export downstream (Figure 9). However, in most anoxic summers, the reservoir became a net source of TOC and TP downstream, meaning that inflowing TOC and TP—as well as TOC and TP that were previously retained in the reservoir sediments—were released and transported out of the reservoir (Figure 8a,g). Consequently, the reservoir exported a median of 105% of inflowing TOC and 123% of inflowing TP in anoxic conditions (Figure 9). DOC and DRP fluxes largely mirrored the patterns of the total fractions, though DRP had much greater flux downstream overall in anoxic summers than TP (Figure 8b,g,h).

The reservoir was a net source of TN, DIN, and NH_4^+ downstream even in oxic conditions, but this export significantly increased when the hypolimnion became anoxic in summer (Figure 8c,d,e). The only fraction of N that did not exhibit higher downstream export during anoxic conditions was NO_3^- (Figure 8f). During anoxic conditions, ~100% of inflowing NO_3^- was removed due to sediment denitrification, whereas in oxic conditions, some of this NO_3^- was exported downstream along with additional NO_3^- that originated from nitrified NH_4^+ in the reservoir (Figure 7b). Overall, the reservoir

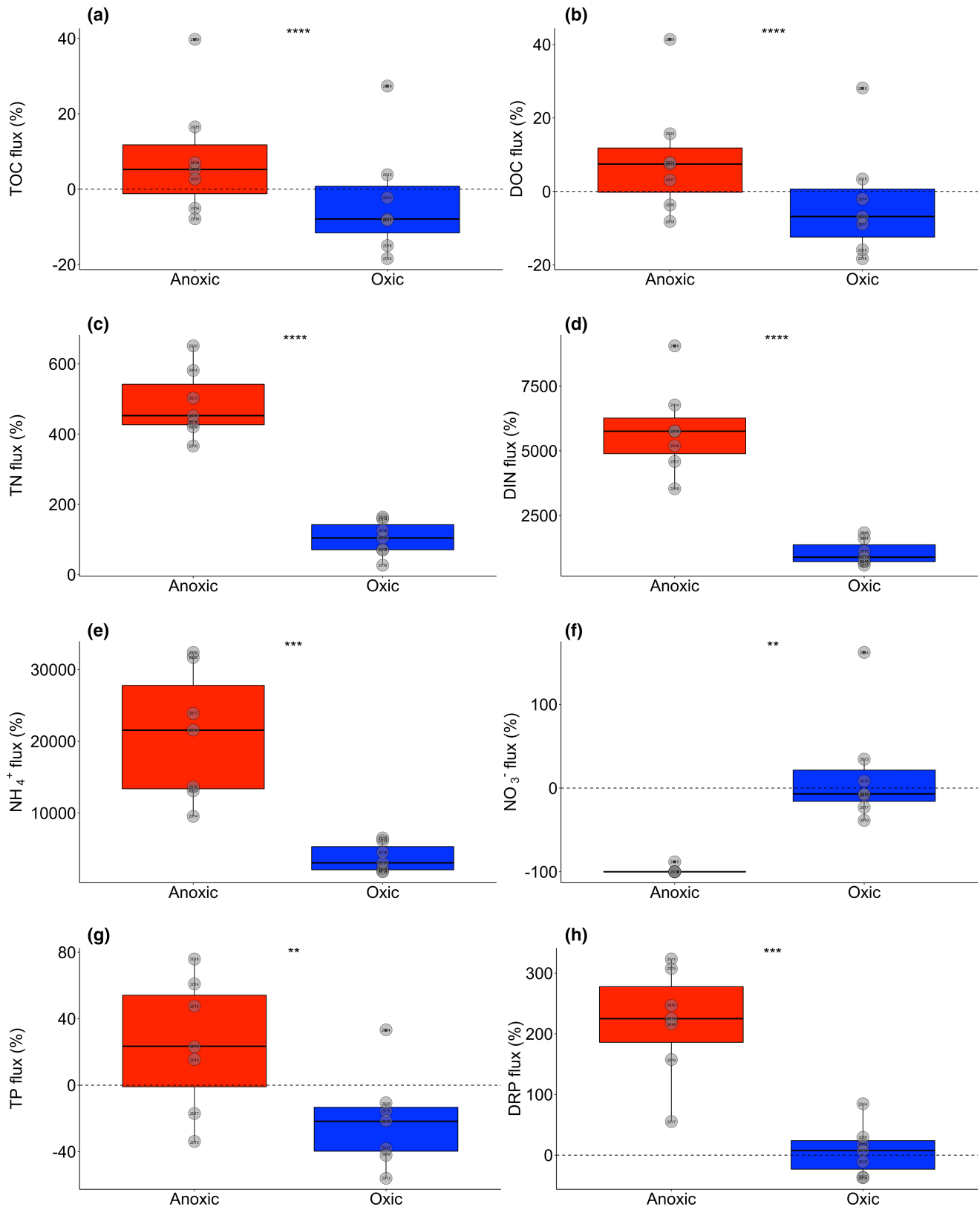
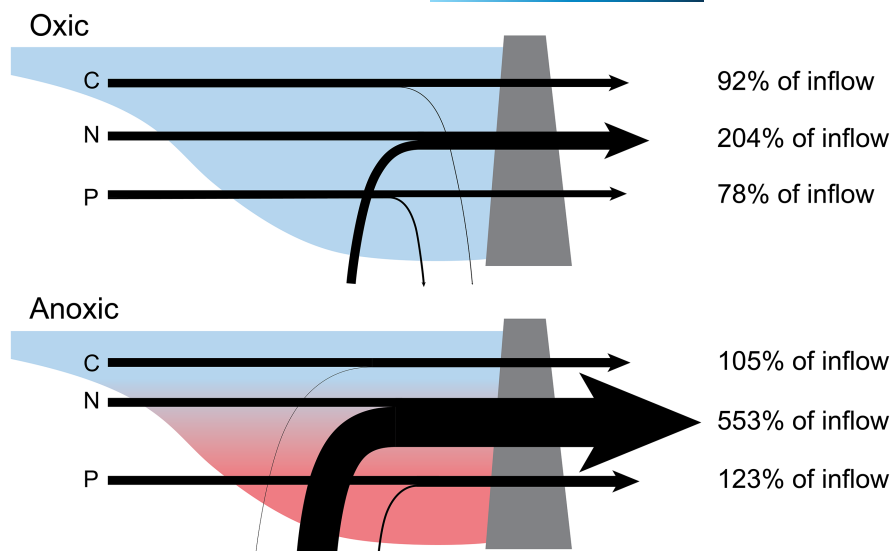


FIGURE 8 Anoxia significantly increased the downstream export of organic carbon, nitrogen, and phosphorus. Percent downstream export (% flux) of total organic carbon (TOC; a), dissolved organic carbon (DOC; b), total nitrogen (TN; c), dissolved inorganic nitrogen (DIN; d), ammonium (NH_4^+ ; e), nitrate (NO_3^- ; f), total phosphorus (TP; g), and dissolved reactive phosphorus (DRP; h) inputs into Falling Creek Reservoir for anoxic (red) and oxic (blue) model scenarios during the stratified period (July 15–October 1) for all years of this study. Flux values of 0 (denoted by dashed horizontal lines) indicated that the reservoir inputs balanced exports; flux values <0 indicated that the reservoir was a net sink of C, N, or P; and flux values >0 indicated that the reservoir was a net source of C, N, or P downstream. The grey points are the median values from each of the 7 years. The asterisks denote the p-values from paired t-tests comparing the median summer retention in anoxic and oxic scenarios: **** $p < .0001$, *** $p < .001$, and ** $p < .01$ (see Table S5 for statistics). Note varying y-axes among panels

FIGURE 9 Median summer downstream export of total organic carbon (C), total nitrogen (N), and total phosphorus (P) inputs under oxic (top) and anoxic (bottom) conditions. The “% of inflow” value represents the percent of inflowing C, N, and P into the reservoir that is exported downstream. A value of 100% indicates that reservoir inputs balanced exports; values <100% indicated that the reservoir was a net sink of C, N, or P; and values >100% indicated that the reservoir was a net source of C, N, or P downstream. Arrow widths are scaled to be proportional to the median downstream export of each element



exported 204% of inflowing TN in summer oxic conditions and 553% in anoxic conditions (Figure 9).

Aggregated across the 7 years, FCR served as a small net sink of POC, PON, and POP in its sediments in both oxic and anoxic model scenarios. All particulate organic fractions exhibited significantly higher annual burial rates in anoxic scenarios than oxic scenarios, though the differences were small, especially for POP (Table S6).

4 | DISCUSSION

Our REDOX study provides one of the first comprehensive analyses on the effects of oxygen on multiple fractions of C, N, and P at the whole-ecosystem scale in a freshwater ecosystem. Our unprecedented 7-year field manipulation coupled with ecosystem model simulations reveals that anoxia may decrease the ability of reservoirs to serve as sinks of C, N, and P. Moreover, both the empirical data and model output demonstrate that anoxia resulted in significantly higher summer concentrations of hypolimnetic NH_4^+ , DRP, and DOC and altered dissolved and total stoichiometry by factors of 2–5x. Our integrated field manipulation and modeling study provides important insight on the biogeochemical cycling of these three elements, which are already changing in many freshwaters globally due to human activities (e.g., Maranger et al., 2018; Powers et al., 2015), and likely will change substantially more in the future as the prevalence and duration of anoxia in lakes and reservoirs increase (Jane et al., 2021; Jenny, Francus, et al., 2016; North et al., 2014; Tranvik et al., 2009). Below, we first examine the effects of anoxia on each elemental cycle separately, then their combined stoichiometry, and ultimately whole-ecosystem biogeochemical processing and fate.

4.1 | Hypolimnetic carbon and nutrient chemistry

This study provides an answer to the critical question of how increased anoxia will affect OC cycling at the whole-ecosystem scale

(Brothers et al., 2014; Carey et al., 2018; Mendonça et al., 2017; Peter et al., 2016; Sobek et al., 2009). The shift in reservoir OC cycling in response to anoxia is the consequence of changes in three linked processes: POC burial, DOC mineralization, and DOC release from the sediments. Under anoxic conditions, POC burial increased slightly, DOC mineralization rates were low, and DOC release from the sediments to the water column was 2x higher than in oxic conditions (Figure 7a; Table S6). Under oxic conditions, DOC mineralization rates, while higher than in anoxic conditions (Figure 7; Figure S5), were still an order of magnitude lower than the rate of hydrologic flushing. The net outcome of these three processes was a substantial difference in OC retention in the reservoir during oxic versus anoxic conditions. Under oxic conditions, the reservoir served as a net sink of DOC and TOC, with up to 18% of inflowing DOC and TOC retained in a summer (Figure 8a,b). Under anoxic conditions, the decrease in net retention of inflowing DOC and TOC more than offset the slight increase in POC burial, and nearly all of the inflowing DOC and TOC was exported downstream (as indicated by 0% or positive flux in Figure 8a,b). In five of the 7 years, FCR even became a net exporter of TOC and DOC in the anoxic scenario (Figure 8a,b), meaning that both inflowing TOC and DOC, and likely legacy TOC and DOC that were previously buried in sediments, were released and transported out of the reservoir.

The finding that anoxia simultaneously decreased the reservoir's role as a DOC sink yet increased its role as a POC sink may explain some of the conflicting results that emerged from previous studies that focused on only one OC fraction. First, our study supports past work that observed increasing hypolimnetic DOC concentrations in anoxic conditions, suggesting that anoxia decreases the freshwater OC sink (Brothers et al., 2014; Mendonça et al., 2017; Peter et al., 2016). The increasing hypolimnetic DOC concentrations have been attributed to both reductive dissolution of iron-bound OC complexes in the sediments during anoxia (Peter et al., 2016; Peter et al., 2017; Skoog & Arias-Esquivel, 2009) and decreased mineralization rates in anoxic conditions (Bastviken et al., 2004; Sobek et al., 2009). Our calibrated ecosystem model indicates that

both processes are important, but that the much higher hypolimnetic DOC concentrations in anoxic conditions in FCR were primarily due to sediment release (Figure 7a). At the same time, our work also supports laboratory microcosm and sediment core studies that observed lower POC mineralization rates in anoxic than in oxic conditions (Bastviken et al., 2004; Sobek et al., 2009). In FCR, mean summer POC hydrolysis rates in the hypolimnion were five orders of magnitude lower in anoxic than oxic conditions (Figure 7a; Figure S5), enabling slightly greater POC burial in anoxic than oxic conditions. Altogether, our work indicates that using an ecosystem model to simultaneously track both concentrations and rates of the major processes affecting dissolved, particulate, and total pools of OC is needed to understand the full effects of oxygen on OC cycling, as different fractions have different responses to anoxia.

Nitrogen was the most sensitive of the three focal elements to anoxia, with an NH_4^+ -dominated TN budget that increased dramatically during anoxic conditions. The dominant mechanism driving the NH_4^+ increase in anoxic conditions was the approximately 4x higher rates of ammonification and sediment release than those observed in oxic conditions (Figure 7b). Anammox and nitrification rates were very low in anoxic conditions (Figure 7b, Figure S5), enabling NH_4^+ to accumulate in the hypolimnion during anoxia. In oxic conditions, nitrification rates were unable to balance sediment fluxes, resulting in much lower but still noticeable increases in summer NH_4^+ concentrations (Figure 4g). As a result, the reservoir functioned as an NH_4^+ source downstream regardless of hypolimnetic oxygen availability, though anoxia increased downstream fluxes by 5x relative to oxic conditions, on average. The high sediment NH_4^+ fluxes, even in oxic conditions, indicate that FCR has a large sediment NH_4^+ pool, which is likely due to historical agriculture in the catchment (Gerling et al., 2016). Until agricultural abandonment in the 1930s, most of FCR's catchment was farmland (Gerling et al., 2016). Even though the catchment did not experience industrial farming, agriculture can have century-long effects on soil properties, erosion, and ecosystem functioning (Cusack et al., 2013; Foster et al., 2003), resulting in a large pool of NH_4^+ that can be recycled between the hypolimnion and sediments for many years before eventual export (Ahlgren et al., 1994; Gerling et al., 2016).

Following expectation, hypolimnetic NO_3^- concentrations were significantly higher in oxic conditions than anoxic conditions. Despite an increase in NO_3^- during oxic conditions, the dominance of NH_4^+ over NO_3^- in the DIN pool (due to high NH_4^+ sediment fluxes even in oxic conditions; Figure 7b) resulted in overall similar patterns for TN and NH_4^+ (Figure 5c,d,e). We initially anticipated that an increase in NO_3^- in oxic conditions could balance an increase in NH_4^+ in anoxic conditions, thereby resulting in similar DIN concentrations regardless of oxygen level, but low nitrification rates prevented large increases in NO_3^- from occurring in oxic conditions (Figure 7b). Long-term water chemistry monitoring of FCR shows much lower summer NO_3^- concentrations over time relative to NH_4^+ (Figure 3e,f), and thus modeled results follow observations.

Altogether, anoxia significantly decreased FCR's role as a NH_4^+ sink and simultaneously increased its role as an NO_3^- sink (Figure 8e,f), to the extent that ~100% of inflowing NO_3^- was removed via denitrification. A previous study reported an average TN retention rate of 26% (and up to 78%) of inputs for agricultural reservoirs in the U.S. (Powers et al., 2015). It would be expected that FCR, which is located in a forested catchment, would have much higher TN retention than agricultural reservoirs because of its lower external TN loads; however, FCR's high export of NH_4^+ resulted in the reservoir serving as a source of TN downstream regardless of hypolimnetic oxygen availability (Figure 9). We anticipate that a greater duration and prevalence of hypolimnetic anoxia in lakes and reservoirs could increase freshwater NO_3^- retention, while decreasing TN retention if a waterbody's DIN pool is dominated by NH_4^+ , as in FCR.

Summer hypolimnetic DRP concentrations were approximately 3x higher in anoxic conditions than oxic conditions (Figure 5h). DRP cycling was primarily controlled by sediment fluxes (Figure 7c), which encompassed both release from metal complexes and sediment organic matter into the water column. Our observation of 2.2x higher sediment release rates of DRP in anoxic than oxic conditions (Figure 7c) follows decades of work that have observed similar patterns of increased P fluxes during anoxia (Boström et al., 1988; Mortimer, 1971; Nürnberg, 1987; Rydin, 2000; Søndergaard et al., 2003).

A novel component of our study is that we simultaneously quantified both dissolved and total pools of P at the whole-ecosystem scale in our model simulations, allowing us to disentangle the responses of different P fractions to anoxia. While DRP concentrations tripled in response to anoxia, TP concentrations only increased by 1.6x (Figure 5g,h), indicating a lower sensitivity of particulate P than DRP to hypolimnetic oxygen conditions in FCR. This result is supported by the negligible (albeit statistically significant) response of POP to changes in oxygen availability (Table S6). Consequently, we expect that the effects of anoxia on reservoir TP dynamics are dependent on the proportion of dissolved P versus particulate P within the TP pool. If the hypolimnetic DRP pool comprises a sizeable proportion of TP, as observed in FCR (median of $11 \pm 1\%$), then TP retention will likely be sensitive to anoxia (e.g., Figure 9), but if DRP is lower, then TP cycling may be more resilient to anoxia.

4.2 | Shifts in stoichiometry in response to anoxia

The substantial difference in stoichiometric ratios between anoxic and oxic conditions has important implications for understanding how anoxia affects the ecosystem functioning of lakes and reservoirs. Because anoxia increased hypolimnetic NH_4^+ concentrations more than any other dissolved or total fraction in this study, and NH_4^+ dominated both the dissolved and total N pools, any stoichiometric ratios that included NH_4^+ , DIN, or TN exhibited large shifts during anoxia (Figure 6). The significantly higher TN:TP and DIN:DRP ratios observed during anoxia will likely affect water

quality and food web structure (Figure 6g,h). Higher N:P ratios favor non-N-fixing cyanobacteria and will shift the composition of other taxa in phytoplankton community based on their N and P requirements (Reynolds, 2006), as phytoplankton can access hypolimnetic nutrients via multiple mechanisms (Cottingham et al., 2015). In contrast, the significantly lower TOC:TN, TOC:TP, DOC:DIN, DOC:NH₄⁺, and DOC:DRP ratios during anoxia (Figure 6a–d,f) could increase organic matter mineralization rates (e.g., Coble et al., 2015).

Our results both support and contradict earlier studies that measured freshwater stoichiometry across many waterbodies. Similar to an analysis of >27,000 freshwater samples from U.S. waterbodies (Helton et al., 2015), we observed inverse relationships between NO₃[−] versus NH₄⁺ concentrations and DOC versus DIN concentrations (Figure 6). Our study provides experimental evidence to support the hypothesis that redox gradients are a major driver of NO₃[−]:NH₄⁺ and DOC:DIN ratios, which will increase in oxic conditions and decrease in anoxic conditions (Helton et al., 2015). On the other hand, our work finds only partial support for earlier findings of lower TOC:TP and TN:TP ratios in reservoirs than natural lakes in an analysis of ~1000 U.S. waterbodies, which was attributed in part to a greater incidence of anoxia in reservoirs (Maranger et al., 2018). Median TOC:TP and TN:TP ratios in the reservoirs of that study were 417 and 38, respectively, which are similar to the ratios observed in FCR (Figure 6b,g). While anoxia decreased TOC:TP ratios (Figure 6b), it also increased TN:TP ratios (Figure 6g), suggesting that anoxia is not responsible for all differences in stoichiometry between reservoirs and natural lakes. Our results indicate that individual waterbodies' responses to anoxia may be dependent on the dominance of NO₃[−] versus NH₄⁺ in their DIN pool prior to the onset of anoxia: if NO₃[−] dominates, then TN:TP ratios will likely decrease with anoxia, while if NH₄⁺ dominates, then TN:TP ratios will likely increase. In general, most lakes tend to have higher NO₃[−] than NH₄⁺ concentrations (Leoni et al., 2018; Quirós, 2003), suggesting that anoxia may result in lower TN:TP ratios in most waterbodies.

4.3 | Opportunities and challenges of our whole-ecosystem approach

Our coupled field manipulation and modeling study—REDOX—provided a powerful approach for quantifying freshwater ecosystem responses to anoxia. By focusing on the same reservoir experiencing different oxygen conditions over multiple years, we were able to isolate the effects of oxygen on C, N, and P cycling without having to disentangle ecosystem-specific responses (e.g., if we were comparing across multiple waterbodies). Ideally, we would have run the REDOX field manipulation with multiple summers of continuous oxygenation and multiple summers of no oxygenation to contrast hypolimnetic conditions. However, we were constrained in our manipulation as the reservoir was an active drinking water source during the study, necessitating us to activate the oxygenation system every summer

for the preservation of water quality. Consequently, we used the calibrated ecosystem model to simulate the biogeochemistry of continuously oxygenated and never-oxygenated scenarios, which uniquely enabled us to compare the effect of oxygenation while holding all other factors constant, such as temperature (Figure 4a). The similar biogeochemical responses to anoxia between the non-oxygenated versus oxygenated field data and the anoxic versus oxic model scenarios, respectively, support our integrated study approach and the robustness of our findings (e.g., Figure 5; Figure S2).

The simulation model provided insights to reservoir responses to anoxia that would have been challenging to glean from field observations alone. We used the model to calculate whole-ecosystem rates that are impossible to measure in the field (e.g., daily POC burial), determine the relative importance of different processes for biogeochemical budgets, and quantify how processes changed in anoxic versus oxic conditions. While the model's biogeochemical rates were determined from automated optimization and calibration of numerical simulation parameters, they fall within reasonable ranges of biogeochemical rates observed in the field, supporting our model results. For example, hypolimnetic sediment flux chamber measurements that were collected in FCR in summer 2018 measured a mean sediment oxygen demand of ~20 mmol m^{−2} day^{−1} (range 8–37.5 mmol m^{−2} day^{−1}), which compares well with our calibrated hypolimnetic flux of 29 mmol m^{−2} day^{−1} (Krueger et al., 2020). That study also measured NH₄⁺, DRP, and DOC fluxes from the sediment into the water column as the chambers became anoxic, with calculated release rates up to 2.7 mmol NH₄⁺ m^{−2} day^{−1}, 0.01 mmol DRP m^{−2} day^{−1}, and 14 mmol DOC m^{−2} day^{−1} (Supporting Information Text 1). These numbers are consistent with our maximum calibrated rates of 2.8 mmol NH₄⁺ m^{−2} day^{−1} and 0.02 mmol DRP m^{−2} day^{−1} (Carey, Thomas, & Hanson, 2022). Our maximum calibrated rate for DOC sediment flux, 1.4 mmol DOC m^{−2} day^{−1}, is an order of magnitude lower than the field data, suggesting that our modeled sediment flux rate of DOC was likely conservative.

We note several limitations to our study that should be considered. First, FCR is a small reservoir (0.119 km²). However, its size is representative of many U.S. reservoirs: 72% of the reservoirs in the U.S. National Inventory of Dams have the same surface area or smaller (NID, 2021). Second, we focused on the hypolimnion of FCR as a reactor in which we could isolate coupled biogeochemical processes occurring during summer stratification, when C, N, and P processing rates are usually at their highest due to warm temperatures. This focus on the hypolimnion precluded the analysis of other important processes that can have large effects on biogeochemical cycling in the epilimnion (e.g., photodegradation). Third, FCR has a hypolimnetic withdrawal, which results in increased downstream export of hypolimnetic water from the reservoir. While export of hypolimnetic water is limited in many naturally formed lakes, hypolimnetic withdrawals are very common in reservoirs that provide drinking water, hydropower, and flood risk protection (Hayes et al., 2017), which represent a large proportion of the reservoirs in the U.S. (NID, 2021). Fourth, similar to many other lake modeling studies (e.g., Farrell et al., 2020; Kara et al., 2012; Ward et al., 2020),

it was challenging to model NO_3^- and DRP. For these solutes in particular, most of the variation in observations was within the limits of quantitation (Supporting Information Text 2), indicating that the model should not necessarily be penalized for the low performance in its evaluation metrics. Despite these challenges, the N and P parameters used for modeling FCR are consistent with other applications of the GLM-AED for other lakes (e.g., Farrell et al., 2020; Kara et al., 2012; Ward et al., 2020), and overall, we were generally able to recreate observed physical, chemical, and biological dynamics in both the epilimnion and hypolimnion (Figure 3; Figures S3 and S4). Moreover, the similar results between the anoxic versus oxic model scenarios and the field data from contrasting non-oxygenated versus oxygenated summer days (Figure 5; Figure S2) support our approach and overall results.

5 | CONCLUSIONS

The duration, prevalence, and magnitude of anoxia in the bottom waters of lakes and reservoirs are increasing globally (Butcher et al., 2015; Jane et al., 2021; Jenny, Francus, et al., 2016). While low oxygen conditions are typically thought of as a response to land use and climate change (Jane et al., 2021; Jenny, Normandeau, et al., 2016), our analysis demonstrates that low oxygen can also be a driver of major changes to freshwater biogeochemical cycling.

Importantly, our work indicates that anoxia may alter the ability of freshwater ecosystems to serve as sinks of C, N, and P in the landscape. Consequently, while hypolimnetic anoxia is a result of increased C, N, and P loading into a waterbody, we also show that it may serve as an intensifying feedback that increases anoxia in downstream waterbodies. This is evident in our study, as we found significantly higher fluxes of C, N, and P downstream when FCR was exhibiting anoxic versus oxic conditions during the summer. Anoxia thus has the potential to both degrade the water quality of a low-oxygen lake or reservoir as well as its downstream waterbodies. While more data are needed to evaluate the consequences of this feedback on downstream water quality, we hypothesize that it could be an important process affecting water quality in some freshwater ecosystems and necessitate greater treatment of water extracted for drinking. Given the vital role that inland waters play in removing C, N, and P from downstream export (Harrison et al., 2009; Maranger et al., 2018; Powers et al., 2016), an increased prevalence and duration of anoxia in lakes and reservoirs will likely have major effects on global freshwater C, N, and P budgets as well as water quality and ecosystem functioning.

AUTHOR CONTRIBUTIONS

Conceptualization: CCC, PCH, MES; Data curation: CCC, ABG, AGH, ASL, MEL, RPM, HLW, WMW, BRN; Formal analysis: CCC, PCH, RQT; Investigation: CCC, ABG, AGH, ASL, MEL, RPM, HLW, WMW, BRN, MES; Methodology: CCC, PCH, RQT; Project administration: CCC; Software: RQT; Visualization: CCC, ASL, RPM, WMW, AGH,

HLW; Supervision: CCC, MES; Writing-original draft: CCC, MEL, BRN, AGH; Writing-review & editing: CCC, PCH, RQT, ABG, AGH, ASL, MEL, RPM, HLW, WMW, BRN, MES.

ACKNOWLEDGMENTS

We thank the Western Virginia Water Authority, especially Jamie Morris, for their long-term partnership and support. We thank Paul Gantzer, John Little, Jonathan Doubek, Kathryn Krueger, Zackary Munger, and François Birgand for assistance with REDOX, and many field and lab assistants past and present in the Virginia Tech Reservoir Group. This work benefitted from discussions with Nelson Hairston, Jr., Emil Rydin, and Kathleen Weathers and constructive feedback from three reviewers. This study was financially supported by the National Science Foundation (DEB-1753639, DEB-1753657, CNS-1737424, DBI-1933016, DBI-1933102, DGE-1651272), Fralin Life Sciences Institute, Institute for Critical Technology and Applied Science, and Virginia Tech Global Change Center.


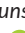






CONFLICT OF INTEREST

The authors declare that they have no competing interests.

DATA AVAILABILITY STATEMENT

All data and code are available in the Environmental Data Initiative repository (Carey et al., 2019; Carey et al., 2020; Carey, Hounshell, et al., 2021; Carey, Lewis, et al., 2021; Carey, Thomas, & Hanson, 2022; Carey, Wander, et al., 2021; Carey, Wynne, et al., 2021) and Zenodo repository (Carey, Thomas, McClure, et al., 2022).

ORCID

Cayelan C. Carey  <https://orcid.org/0000-0001-8835-4476>
 Paul C. Hanson  <https://orcid.org/0000-0001-8533-6061>
 R. Quinn Thomas  <https://orcid.org/0000-0003-1282-7825>
 Alexandra B. Gerling  <https://orcid.org/0000-0001-5280-6709>
 Alexandria G. Hounshell  <https://orcid.org/0000-0003-1616-9399>
 Abigail S. L. Lewis  <https://orcid.org/0000-0001-9933-4542>
 Mary E. Lofton  <https://orcid.org/0000-0003-3270-1330>
 Ryan P. McClure  <https://orcid.org/0000-0001-6370-3852>
 Heather L. Wander  <https://orcid.org/0000-0002-3762-6045>
 Whitney M. Woelmer  <https://orcid.org/0000-0001-5147-3877>
 B. R. Niederlehner  <https://orcid.org/0000-0002-6933-336X>
 Madeline E. Schreiber  <https://orcid.org/0000-0002-1858-7730>

REFERENCES

- Ahlgren, I., Waara, T., Vrede, K., & Soerensson, F. (1994). Nitrogen budgets in relation to microbial transformations in lakes. *Ambio*, 23, 367–377.
- APHA. (2017). *Standard methods for the examination of water and wastewater* (23rd ed.). American Public Health Association, American Water Works Association.
- Bartosiewicz, M., Przytulska, A., Lapierre, J.-F., Laurion, I., Lehmann, M. F., & Maranger, R. (2019). Hot tops, cold bottoms: Synergistic climate warming and shielding effects increase carbon burial in lakes. *Limnology and Oceanography-Letters*, 4, 132–144.
- Bastviken, D., Cole, J., Pace, M., & Tranvik, L. (2004). Methane emissions from lakes: Dependence of lake characteristics, two regional

- assessments, and a global estimate. *Global Biogeochemical Cycles*, 18, GB4009.
- Beaulieu, J. J., Smolenski, R. L., Nietch, C. T., Townsend-Small, A., Elovitz, M. S., & Schubauer-Berigan, J. P. (2014). Denitrification alternates between a source and sink of nitrous oxide in the hypolimnion of a thermally stratified reservoir. *Limnology and Oceanography*, 59, 495–506.
- Beusen, A. H. W., Bouwman, A. F., Van Beek, L. P. H., Mogollón, J. M., & Middelburg, J. J. (2016). Global riverine N and P transport to ocean increased during the 20th century despite increased retention along the aquatic continuum. *Biogeosciences*, 13, 2441–2451.
- Beutel, M., Burley, N., & Culmer, K. (2006). Quantifying the effects of water velocity and oxygen on sediment oxygen demand. *Hydrological Sciences & Technology*, 22, 271–228.
- Beutel, M. W. (2003). Hypolimnetic anoxia and sediment oxygen demand in California drinking water reservoirs. *Lake and Reservoir Management*, 19, 208–221.
- Boström, B., Andersen, J. M., Fleischer, S., & Jansson, M. (1988). Exchange of phosphorus across the sediment-water interface. *Hydrobiologia*, 170, 229–244.
- Brett, M. T., Ahopelto, S. K., Brown, H. K., Brynestad, B. E., Butcher, T. W., Coba, E. E., Curtis, C. A., Dara, J. T., Doeden, K. B., Evans, K. R., Fan, L., Finley, J. D., Garguilo, N. J., Gebreyesus, S. M., Goodman, M. K., Gray, K. W., Grinnell, C., Gross, K. L., Hite, B. R. E., ... Arhonditsis, G. B. (2016). The modeled and observed response of Lake Spokane hypolimnetic dissolved oxygen concentrations to phosphorus inputs. *Lake and Reservoir Management*, 32, 246–258.
- Brothers, S., Köhler, J., Attermeyer, K., Grossart, H. P., Mehner, T., Meyer, N., Scharnweber, K., & Hilt, S. (2014). A feedback loop links brownification and anoxia in a temperate, shallow lake. *Limnology and Oceanography*, 59, 1388–1398.
- Bruce, L., Frassl, M., Arhonditsis, G., Gal, G., Hamilton, D., Hanson, P., Hetherington, A., Melack, J., Read, J., Rinke, K., Rigosi, A., Trolle, D., Winslow, L., Adrian, R., Ayala Zamora, A., Bocaniov, S., Boehrer, B., Boon, C., Brookes, J., & Hipsey, M. (2018). A multi-lake comparative analysis of the General Lake model (GLM): Stress-testing across a global observatory network. *Environmental Modelling and Software*, 102, 274–291.
- Butcher, J. B., Nover, D., Johnson, T. E., & Clark, C. M. (2015). Sensitivity of lake thermal and mixing dynamics to climate change. *Climatic Change*, 129, 295–305.
- Carey, C. C., Doubek, J. P., McClure, R. P., & Hanson, P. C. (2018). Oxygen dynamics control the burial of organic carbon in a eutrophic reservoir. *Limnology and Oceanography Letters*, 3, 293–301.
- Carey, C. C., Doubek, J. P., Wynne, J. H., & Niederlehner, B. R. (2020). Dissolved silica time series for Beaverdam Reservoir, Carvins Cove Reservoir, Claytor Lake, Falling Creek Reservoir, Gatewood Reservoir, Smith Mountain Lake, and Spring Hollow Reservoir in southwestern Virginia, USA during 2014, ver 1. *Environmental Data Initiative Repository*. <https://doi.org/10.6073/pasta/353aa34bedfd68800c12275633811341>
- Carey, C. C., Hounshell, A. G., Lofton, M. E., Birgand, B., Bookout, B. J., Corrigan, R. S., Gerling, A. B., McClure, R. P., & Woelmer, W. M. (2021). Discharge time series for the primary inflow tributary entering Falling Creek Reservoir, Vinton, Virginia, USA 2013–2021, ver 7. *Environmental Data Initiative Repository*. <https://doi.org/10.6073/pasta/8d22a432aac5560b0f45aa1b21ae4746>
- Carey, C. C., Lewis, A. S., McClure, R. P., Gerling, A. B., Chen, S., Das, A., Doubek, J. P., Howard, D. W., Lofton, M. E., Hamre, K. D., & Wander, H. L. (2021). Time series of high-frequency profiles of depth, temperature, dissolved oxygen, conductivity, specific conductivity, chlorophyll a, turbidity, pH, oxidation-reduction potential, photosynthetic active radiation, and descent rate for Beaverdam Reservoir, Carvins Cove Reservoir, Falling Creek Reservoir, Gatewood Reservoir, and Spring Hollow Reservoir in southwestern Virginia, USA 2013–2020, ver 11. *Environmental Data Initiative Repository*. <https://doi.org/10.6073/pasta/5448f9d415fd09e0090a46b9d4020ccc>
- Carey, C. C., Thomas, R. Q., & Hanson, P. C. (2022). General Lake Model-Aquatic EcoDynamics model parameter set for Falling Creek Reservoir, Vinton, Virginia, USA 2013–2019 ver 1. *Environmental Data Initiative Repository*. <https://doi.org/10.6073/pasta/9f7d037d9a133076a0a0d123941c6396>
- Carey, C. C., Thomas, R. Q., McClure, R. P., Hounshell, A. G., Woelmer, W. M., Wander, H. L., & Lewis, A. S. L. (2022). CareyLabVT/FCR-GLM: FCR GLM-AED model, data, and code for the paper “Anoxia decreases the magnitude of the carbon, nitrogen, and phosphorus sink in freshwaters” in *Global Change Biology* by Carey et al. (v1.2). *Zenodo*. <https://doi.org/10.5281/zenodo.6520742>
- Carey, C. C., Wander, H. L., Woelmer, W. M., Lofton, M. E., Breef-Pilz, A., Doubek, J. P., Gerling, A. B., Hounshell, A. G., McClure, R. P., & Niederlehner, B. R. (2021). Water chemistry time series for Beaverdam Reservoir, Carvins Cove Reservoir, Falling Creek Reservoir, Gatewood Reservoir, and Spring Hollow Reservoir in southwestern Virginia, USA 2013–2020, ver 8. *Environmental Data Initiative Repository*. <https://doi.org/10.6073/pasta/8d83ef7ec202eca9192e3da6dd34a4e0>
- Carey, C. C., Woelmer, W. M., Maze, J. T., & Hounshell, A. G. (2019). Manually-collected discharge data for multiple inflow tributaries entering Falling Creek Reservoir and Beaverdam Reservoir, Vinton, Virginia, USA in 2019, ver 4. *Environmental Data Initiative Repository*. <https://doi.org/10.6073/pasta/4d8e7b7bedbc6507b307ba2d5f2cf9a2>
- Carey, C. C., Wynne, J. H., Wander, H. L., McClure, R. P., Farrell, K. J., Breef-Pilz, A., Doubek, J. P., Gerling, A. B., Hamre, K. D., Hounshell, A. G., Lewis, A. S., Lofton, M. E., & Woelmer, W. M. (2021). Secchi depth data and discrete depth profiles of photosynthetically active radiation, temperature, dissolved oxygen, and pH for Beaverdam Reservoir, Carvins Cove Reservoir, Falling Creek Reservoir, Gatewood Reservoir, and Spring Hollow Reservoir in southwestern Virginia, USA 2013–2020, ver 8. *Environmental Data Initiative Repository*. <https://doi.org/10.6073/pasta/3e9f27971e353ca80840b5e99a67d0c>
- Coble, A., Marcarelli, A., & Kane, E. (2015). Ammonium and glucose amendments stimulate dissolved organic matter mineralization in a Lake Superior tributary. *Journal of Great Lakes Research*, 41, 801–807.
- Cole, J. J. (2013). Freshwater ecosystems and the carbon cycle. In O. Kinne (Ed.), *Excellence in ecology* (Vol. 18, pp. 95–106). International Ecology Institute.
- Cottingham, K. L., Ewing, H. A., Greer, M. L., Carey, C. C., & Weathers, K. C. (2015). Cyanobacteria as biological drivers of lake nitrogen and phosphorus cycling. *Ecosphere*, 6, art1. <https://doi.org/10.1890/ES14-00174.1>
- Cusack, D. F., Chadwick, O. A., Ladefoged, T., & Vitousek, P. M. (2013). Long-term effects of agriculture on soil carbon pools and carbon chemistry along a Hawaiian environmental gradient. *Biogeochemistry*, 112, 229–243.
- Dillon, P. J., & Molot, L. A. (1997). Dissolved organic and inorganic carbon mass balances in Central Ontario lakes. *Biogeochemistry*, 36, 29–42.
- Downes, M. T. (1987). Aquatic nitrogen transformations at low oxygen concentrations. *Applied and Environmental Microbiology*, 54, 172–175.
- Downing, J. A., Prairie, Y. T., Cole, J. J., Duarte, C. M., Tranvik, L. J., Striegl, R. G., McDowell, W. H., Kortelainen, P., Caraco, N. F., Melack, J. M., & Middelburg, J. J. (2006). The global abundance and size distribution of lakes, ponds, and impoundments. *Limnology and Oceanography*, 51, 2388–2397.
- Farrell, K. J., Ward, N. K., Krinos, A. I., Hanson, P. C., Daneshmand, V., Figueiredo, R. J., & Carey, C. C. (2020). Ecosystem-scale nutrient cycling responses to increasing air temperatures vary with lake trophic state. *Ecological Modelling*, 430, 109134.

- Foster, D., Swanson, F., Aber, J., Burke, I., Brokaw, N., Tilman, D., & Knapp, A. (2003). The importance of land-use legacies to ecology and conservation. *Bioscience*, 53, 77–88.
- Frindte, K., Allgaier, M., Grossart, H.-P., & Eckert, W. (2015). Microbial response to experimentally controlled redox transitions at the sediment water interface. *PLoS ONE*, 10, e0143428.
- Gerling, A., Browne, R., Gantzer, P., Mobley, M., Little, J., & Carey, C. (2014). First report of the successful operation of a side stream supersaturation hypolimnetic oxygenation system in a eutrophic, shallow reservoir. *Water Research*, 67, 129–143.
- Gerling, A. B., Munger, Z. W., Doubek, J. P., Hamre, K. D., Gantzer, P. A., Little, J. C., & Carey, C. C. (2016). Whole-catchment manipulations of internal and external loading reveal the sensitivity of a century-old reservoir to hypoxia. *Ecosystems*, 19, 555–571.
- Hansen, N. (2016). The CMA evolution strategy: A tutorial. ArXiv 160400772. <https://arxiv.org/abs/1604.00772>
- Hanson, P. C., Pace, M. L., Carpenter, S. R., Cole, J. J., & Stanley, E. H. (2015). Integrating landscape carbon cycling: Research needs for resolving organic carbon budgets of lakes. *Ecosystems*, 18, 363–375.
- Harrison, J. A., Maranger, R. J., Alexander, R. B., Giblin, A. E., Jacinthe, P.-A., Mayorga, E., Seitzinger, S. P., Sobota, D. J., & Wollheim, W. M. (2009). The regional and global significance of nitrogen removal in lakes and reservoirs. *Biogeochemistry*, 93, 143–157.
- Hayes, N. M., Deemer, B. R., Corman, J. R., Razavi, N. R., & Strock, K. E. (2017). Key differences between lakes and reservoirs modify climate signals: A case for a new conceptual model. *Limnology and Oceanography-Letters*, 2, 47–62.
- Helton, A. M., Ardón, M., & Bernhardt, E. S. (2015). Thermodynamic constraints on the utility of ecological stoichiometry for explaining global biogeochemical patterns. *Ecology Letters*, 18, 1049–1056.
- Hipsey, M. R. (2022). Modelling Aquatic Eco-dynamics: Overview of the AED modular simulation platform (v0.9.0). Zenodo. <https://doi.org/10.5281/zenodo.6516222>
- Hipsey, M. R., Bruce, L. C., Boon, C., Busch, B., Carey, C. C., Hamilton, D. P., Hanson, P. C., Read, J. S., de Sousa, E., Weber, M., & Winslow, L. A. (2019). A General Lake Model (GLM 3.0) for linking with high-frequency sensor data from the Global Lake Ecological observatory network (GLEON). *Geoscience Model Development*, 12, 473–523.
- Hounshell, A. G., McClure, R. P., Lofton, M. E., & Carey, C. C. (2021). Whole-ecosystem oxygenation experiments reveal substantially greater hypolimnetic methane concentrations in reservoirs during anoxia. *Limnology and Oceanography Letters*, 6, 33–42.
- Jane, S. F., Hansen, G. J. A., Kraemer, B. M., Leavitt, P. R., Mincer, J. L., North, R. L., Pilla, R. M., Stetler, J. T., Williamson, C. E., Woolway, R. I., Arvola, L., Chandra, S., DeGasperi, C. L., Diemer, L., Dunalska, J., Erina, O., Flaim, G., Grossart, H.-P., Hambright, K. D., ... Rose, K. C. (2021). Widespread deoxygenation of temperate lakes. *Nature*, 594, 66–70.
- Jenny, J.-P., Francus, P., Normandeau, A., Lapointe, F., Perga, M.-E., Ojala, A., Schimmelmann, A., & Zolitschka, B. (2016). Global spread of hypoxia in freshwater ecosystems during the last three centuries is caused by rising local human pressure. *Global Change Biology*, 22, 1481–1489.
- Jenny, J.-P., Normandeau, A., Francus, P., Taranu, Z. E., Gregory-Eaves, I., Lapointe, F., Jautzy, J., Ojala, A. E. K., Dorioz, J.-M., Schimmelmann, A., & Zolitschka, B. (2016). Urban point sources of nutrients were the leading cause for the historical spread of hypoxia across European lakes. *Proceedings of the National Academy of Sciences of the United States of America*, 113, 12655.
- Kara, E. L., Hanson, P., Hamilton, D., Hipsey, M. R., McMahon, K. D., Read, J. S., Winslow, L., Dedrick, J., Rose, K., Carey, C. C., Bertilsson, S., da Motta Marques, D., Beversdorf, L., Miller, T., Wu, C., Hsieh, Y.-F., Gaiser, E., & Kratz, T. (2012). Time-scale dependence in numerical simulations: Assessment of physical, chemical, and biological predictions in a stratified lake at temporal scales of hours to months. *Environmental Modelling & Software*, 35, 104–121.
- Kim, C., Nishimura, Y., & Nagata, T. (2006). Role of dissolved organic matter in hypolimnetic mineralization of carbon and nitrogen in a large, monomictic lake. *Limnology and Oceanography*, 51, 70–78.
- Kortelainen, P., Rantakari, M., Pajunen, H., Huttunen, J. T., Mattsson, T., Alm, J., Juutinen, S., Larmola, T., Silvola, J., & Martikainen, P. J. (2013). Carbon evasion/accumulation ratio in boreal lakes is linked to nitrogen. *Global Biogeochemical Cycles*, 27, 363–374.
- Krueger, K. M., Vavrus, C. E., Lofton, M. E., McClure, R. P., Gantzer, P., Carey, C. C., & Schreiber, M. E. (2020). Iron and manganese fluxes across the sediment-water interface in a drinking water reservoir. *Water Research*, 182, 116003.
- Ladwig, R., Hanson, P. C., Dugan, H. A., Carey, C. C., Zhang, Y., Shu, L., Duffy, C. J., & Cobourn, K. M. (2021). Lake thermal structure drives interannual variability in summer anoxia dynamics in a eutrophic lake over 37 years. *Hydrology and Earth System Science*, 25, 1009–1032.
- Lau, M. P., Sander, M., Gelbrecht, J., & Hupfer, M. (2016). Spatiotemporal redox dynamics in a freshwater lake sediment under alternating oxygen availabilities: Combined analyses of dissolved and particulate electron acceptors. *Environmental Chemistry*, 13, 826–837.
- Lehner, B., Liermann, C. R., Revenga, C., Vörösmarty, C., Fekete, B., Crouzet, P., Döll, P., Endejan, M., Frenken, K., Magome, J., Nilsson, C., Robertson, J. C., Rödel, R., Sindorf, N., & Wisser, D. (2011). High-resolution mapping of the world's reservoirs and dams for sustainable river-flow management. *Frontiers in Ecology and the Environment*, 9, 494–502.
- Leoni, B., Patelli, M., Soler, V., & Nava, V. (2018). Ammonium transformation in 14 lakes along a trophic gradient. *Water*, 10, 265. <https://doi.org/10.3390/w10030265>
- Maranger, R., Jones, S. E., & Cotner, J. B. (2018). Stoichiometry of carbon, nitrogen, and phosphorus through the freshwater pipe. *Limnology and Oceanography Letters*, 3, 89–101.
- McDonald, C. P., Stets, E. G., Striegl, R. G., & Butman, D. (2013). Inorganic carbon loading as a primary driver of dissolved carbon dioxide concentrations in the lakes and reservoirs of the contiguous United States. *Global Biogeochemical Cycles*, 27, 285–295.
- Medlyn, B. E., Zaehle, S., De Kauwe, M. G., Walker, A. P., Dietze, M. C., Hanson, P. J., Hickler, T., Jain, A. K., Luo, Y., Parton, W., Prentice, I. C., Thornton, P. E., Wang, S., Wang, Y.-P., Weng, E., Iversen, C. M., McCarthy, H. R., Warren, J. M., Oren, R., & Norby, R. J. (2015). Using ecosystem experiments to improve vegetation models. *Nature Climate Change*, 5, 528–534.
- Mendonça, R., Müller, R. A., Clow, D., Verpoorter, C., Raymond, P., Tranvik, L. J., & Sobek, S. (2017). Organic carbon burial in global lakes and reservoirs. *Nature Communications*, 8, 1694.
- Morris, M. D. (1991). Factorial sampling plans for preliminary computational experiments. *Technometrics*, 33, 161–174.
- Mortimer, C. H. (1971). Chemical exchanges between sediments and water in the Great Lakes—Speculations on probable regulatory mechanisms. *Limnology and Oceanography*, 16, 387–404.
- Munger, Z. W., Carey, C. C., Gerling, A. B., Doubek, J. P., Hamre, K. D., McClure, R. P., & Schreiber, M. E. (2019). Oxygenation and hydrologic controls on iron and manganese mass budgets in a drinking-water reservoir. *Lake and Reservoir Management*, 35, 277–291.
- NID. (2021). U.S. National Inventory of Dams. US Army Corps of Engineers. <https://nid.usace.army.mil/#/>
- North, R. P., North, R. L., Livingstone, D. M., Köster, O., & Kipfer, R. (2014). Long-term changes in hypoxia and soluble reactive phosphorus in the hypolimnion of a large temperate lake: Consequences of a climate regime shift. *Global Change Biology*, 20, 811–823.
- Nürnberg, G. K. (1987). A comparison of internal phosphorus loads in lakes with anoxic hypolimnia. *Limnology and Oceanography*, 32, 1160–1164.

- Nürnberg, G. K. (1988). Prediction of phosphorus release rates from total and reductant-soluble phosphorus in anoxic lake sediments. *Canadian Journal of Fisheries and Aquatic Sciences*, 45, 453–462.
- Peter, S., Agstam, O., & Sobek, S. (2017). Widespread release of dissolved organic carbon from anoxic boreal lake sediments. *Inland Waters*, 7, 151–163.
- Peter, S., Isidorova, A., & Sobek, S. (2016). Enhanced carbon loss from anoxic lake sediment through diffusion of dissolved organic carbon. *Journal of Geophysical Research: Biogeosciences*, 121, 1959–1977.
- Powers, S. M., Bruulsema, T. W., Burt, T. P., Chan, N. I., Elser, J. J., Haygarth, P. M., Howden, N. J. K., Jarvie, H. P., Lyu, Y., Peterson, H. M., Sharpley, A. N., Shen, J., Worrall, F., & Zhang, F. (2016). Long-term accumulation and transport of anthropogenic phosphorus in three river basins. *Nature Geoscience*, 9, 353–356.
- Powers, S. M., Tank, J. L., & Robertson, D. M. (2015). Control of nitrogen and phosphorus transport by reservoirs in agricultural landscapes. *Biogeochemistry*, 124, 417–439.
- Quirós, R. (2003). The relationship between nitrate and ammonia concentrations in the pelagic zone of lakes. *Limnetica*, 22, 37–50.
- R Core Team. (2020). R: A language and environment for statistical computing. Version 3.6.3. R Foundation for Statistical Computing.
- Reynolds, C. S. (2006). *Ecology of phytoplankton* (pp. 145–175). Cambridge University Press.
- Rydin, E. (2000). Potentially mobile phosphorus in Lake Erken sediment. *Water Research*, 34, 2037–2042.
- Rysgaard, S., Risgaard-Petersen, N., Sloth, N., Jensen, K. I. M., & Nielsen, L. P. (1994). Oxygen regulation of nitrification and denitrification in sediments. *Limnology and Oceanography*, 39, 1643–1652.
- Sharma, B., & Ahlert, R. C. (1977). Nitrification and nitrogen removal. *Water Research*, 11, 897–925.
- Skoog, A. C., & Arias-Esquivel, V. A. (2009). The effect of induced anoxia and reoxygenation on benthic fluxes of organic carbon, phosphate, iron, and manganese. *Science of the Total Environment*, 407, 6085–6092.
- Soares, L. M. V., & Calijuri, M. D. C. (2021). Deterministic modelling of freshwater lakes and reservoirs: Current trends and recent progress. *Environmental Modelling & Software*, 144, 105143.
- Sobek, S., Durisch-Kaiser, E., Zurbrugg, R., Wongfun, N., Wessels, M., Pasche, N., & Wehrli, B. (2009). Organic carbon burial efficiency in lake sediments controlled by oxygen exposure time and sediment source. *Limnology and Oceanography*, 54, 2243–2254.
- Søndergaard, M., Jensen, J. P., & Jeppesen, E. (2003). Role of sediment and internal loading of phosphorus in shallow lakes. *Hydrobiologia*, 506, 135–145.
- Sterner, R., & Elser, J. J. (2002). *Ecological stoichiometry: The biology of elements from molecules to the biosphere*. Princeton University Press.
- Toming, K., Kotta, J., Uuemaa, E., Sobek, S., Kutser, T., & Tranvik, L. J. (2020). Predicting lake dissolved organic carbon at a global scale. *Scientific Reports*, 10, 8471.
- Tranvik, L. J., Downing, J. A., Cotner, J. B., Loiselle, S. A., Striegl, R. G., Ballatore, T. J., Dillon, P., Finlay, K., Fortino, K., Knoll, L. B., Kortelainen, P. L., Kutser, T., Larsen, S., Laurion, I., Leech, D. M., McCallister, S. L., McKnight, D. M., Melack, J. M., Overholt, E., ... Weyhenmeyer, G. A. (2009). Lakes and reservoirs as regulators of carbon cycling and climate. *Limnology and Oceanography*, 54, 2298–2314.
- Vachon, D., Langenegger, T., Donis, D., & McGinnis, D. F. (2019). Influence of water column stratification and mixing patterns on the fate of methane produced in deep sediments of a small eutrophic lake. *Limnology and Oceanography*, 64, 2114–2128.
- Verpoorter, C., Kutser, T., Seekell, D. A., & Tranvik, L. J. (2014). A global inventory of lakes based on high-resolution satellite imagery. *Geophysical Research Letters*, 41, 6396–6402.
- Walker, R. R., & Snodgrass, W. J. (1986). Model for sediment oxygen demand in lakes. *Journal of Environmental Engineering*, 112, 25–43.
- Ward, N. K., Steele, B. G., Weathers, K. C., Cottingham, K. L., Ewing, H. A., Hanson, P. C., & Carey, C. C. (2020). Differential responses of maximum versus median chlorophyll-a to air temperature and nutrient loads in an oligotrophic lake over 31 years. *Water Resources Research*, 56, e2020WR027296.
- Wetzel, R. G. (2001). *Limnology: Lake and river ecosystems* (3rd ed.). Academic Press.
- Woolway, R. I., Sharma, S., Weyhenmeyer, G. A., Debolskiy, A., Golub, M., Mercado-Bettin, D., Perroud, M., Stepanenko, V., Tan, Z., Grant, L., Ladwig, R., Mesman, J., Moore, T. N., Shatwell, T., Vanderkelen, I., Austin, J. A., DeGasperi, C. L., Dokulil, M., La Fuente, S., ... Jennings, E. (2021). Phenological shifts in lake stratification under climate change. *Nature Communications*, 12, 2318.
- Xia, Y., Mitchell, K., Ek, M., Sheffield, J., Cosgrove, B., Wood, E., Luo, L., Alonge, C., Wei, H., Meng, J., Livneh, B., Lettenmaier, D., Koren, V., Duan, Q., Mo, K., Fan, Y., & Mocko, D. (2012). Continental-scale water and energy flux analysis and validation for the North American land data assimilation system project phase 2 (NLDAS-2): 1. Intercomparison and application of model products. *Journal of Geophysical Research: Atmospheres*, 117, D03109.
- Zarfl, C., Lumsdon, A. E., Berlekamp, J., Tydecks, L., & Tockner, K. (2015). A global boom in hydropower dam construction. *Aquatic Sciences*, 77, 161–170.

SUPPORTING INFORMATION

Additional supporting information may be found in the online version of the article at the publisher's website.

How to cite this article: Carey, C. C., Hanson, P. C., Thomas, R. Q., Gerling, A. B., Hounshell, A. G., Lewis, A. S. L., Lofton, M. E., McClure, R. P., Wander, H. L., Woelmer, W. M., Niederlehner, B. R., & Schreiber, M. E. (2022). Anoxia decreases the magnitude of the carbon, nitrogen, and phosphorus sink in freshwaters. *Global Change Biology*, 00, 1–21. <https://doi.org/10.1111/gcb.16228>